ACCURATE DETERMINATION OF SOURCE DISINTEGRATION RATES WITH NaI (Tl) GAMMA RAY SPECTROMETER

BY

SA'ADU NASIRU

AUGUST 2006

ACCURATE DETERMINATION OF SOURCE DISINTEGRATION RATES WITH NaI (Tl) GAMMA RAY SPECTROMETER

BY

SA'ADU NASIRU

Physics Department,
Ahmadu Bello University, Zaria, Nigeria.

AUGUST 2006

ACCURATE DETERMINATION OF SOURCE DISINTEGRATION RATES WITH NaI (Tl) GAMMA RAY SPECTROMETER

BY

SA'ADU NASIRU

B .Sc (Hons.) BUK

A Thesis submitted to the Post Graduate School,
Ahmadu Bello University, Zaria, Nigeria.

In partial fulfillment of the requirement for the award of the degree
Master of Science (Physics)

Physics Department,
Ahmadu Bello University, Zaria, Nigeria.

AUGUST 2006

DECLARATION

I Sa'adu Nasiru, hereby declare that this thesis titled "**Accurate Determination Of Source Disintegration Rates With NaI (Tl) Gamma Ray Spectrometer**" is my own work and has not been submitted in any other form for another degree or diploma to any other University or Institution. Information derived from published or unpublished work of other workers has been fully acknowledged in the text.

_____ _____

Sa'adu Nasiru Date

CERTIFICATION

This thesis titled “Accurate Determination Of Source Disintegration Rates With NaI(Tl) Gamma Ray Spectrometer” by SA’ADU NASIRU (MSc/Sci/23565/2000-2001) meets the regulation governing the award of the degree of Master of Science (Physics) of Ahmadu Bello University, Zaria and is approved for its Contribution to knowledge and literacy presentation.

_____	_____
Chairman, Supervisory Committee (Dr. K. Usman)	Date
_____	_____
Member, Supervisory Committee (Dr. S. A. Jonah)	Date
_____	_____
Head of Physics Department (Prof. N. Harriharan)	Date
_____	_____
Dean, Post Graduate School	Date

DEDICATION

This work is dedicated to my beloved parents

Late Alhaji Nasiru Yola

And

Hajiya Aminatu Mahmud

ACKNOWLEDGEMENT

Praise be to The Almighty God, for the guidance and sustenance throughout my academic career. With His mercy I was able to complete this work, I thank Him and seek His forgiveness and support in my subsequent activities.

Special gratitude to The Director Centre for Energy Research and Training (CERT), Prof. I. M. Umar for the opportunity and support given to me to utilize various equipment within the centre. The special nursing and care given to me by my able supervisor Dr. K. Usman can never be forgotten.

I thank for the contribution of my second supervisor Dr. S. A. Jonah and my Head Of Section Dr. G. I. Balogun for the support and advice.

I also acknowledge the support and concern of the Head of Physics Department A.B.U. Zaria, the entire CERT staff, plus my friends and relatives, to mention a few; Prof. I. I. Funtua, Prof. L. A. Dim, Engineer H. A. Adamu, Mallam Abdullahi Alhassan, and Mr. S. Okoh.

The love and moral support given to me by my beloved mother Hajiya Aminatu can never be over emphasized may God reward her with the best of His awards, not forgetting my wife Mariya for her caring support.

ABSTRACT

The aim of this project is to measure the absolute activity (disintegration rates) of gamma sources. The measurement was achieved using a NaI (Tl) spectrometer. The major factors that contribute to uncertainties in the measurement were taken in to account and relevant uncertainties were propagated accordingly. The spectrometre is fully setup for disintegration rates determination.

The spectrometer was calibrated for efficiency at three chosen geometries (10, 14 and 20) cm, the calibration was performed in such a way that significant factors that affect the measurements were considered. The fitted efficiency function coefficients at these chosen levels were obtained and used to write a computer program that calculates the measured absolute activity of sources and its uncertainty easily. The energy gamma range covered by the work is (59 to 1836) KeV.

Therefore the work was able to integrate IAEA Quality Assurance (QA) recommendations, to simplify an accurate methodology for setting up gamma ray spectrometres, using a NaI(Tl) spectrometre. The setup spectrometre used to determine the absolute activity of two old standard calibration sources ^{137}Cs and ^{60}Co, the activity of the ^{137}Cs compared well with that quoted by the manufacturer, while that of ^{60}Co did not agree, its activity was determined to be (31319 ± 2153) Bq, because it leaked prior to this work, it can henceforth be used when needed.

TABLE OF CONTENTS

Title Page	**ii**
Declaration	**iv**
Certification	**v**
Dedication	**vi**
Acknowledgements	**vii**
Abstract	**viii**
Table of Contents	**ix**
List of Tables	**xiv**
List of figures	**xv**
List of Appendices	**xvi**
CHAPTER ONE: INTRODUCTION	**1**
1.1 Introduction	**1**
1.2 Literature Review	**5**
1.3 Justification	**6**
1.4 Objectives	**6**
CHAPTER TWO: GAMMA SPECTROMETRY AND THE SPECTROMETER COMPONENTS	**7**
2.1. Introduction	**7**

2.2. Interactions of Gamma Radiation with Matter **7**

2.2.1. Photoelectric Absorption 8

2.2.2. Compton Scattering 9

2.2.3. Pair Production 11

2.3. Radiation Detectors **11**

2.3.1. Scintillation Detectors 12

2.3.2. Inorganic Scintillators 13

2.3.3. NaI (Tl) Detector 14

2.3.4. Photomultiplier Tubes 15

2.4. Description of the Spectrometer Components **15**

2.4.1. Characteristics of the NaI (Tl) Detector used 16

2.4.2. The Photo Multiplier Tube And Preamplifier 16

2.4.3. The Minibin And Power Supply 16

2.4.4. The Detector Bias Supply 17

2.4.5. The Linear Amplifier 17

2.4.6. The Computer System Unit 17

2.5. The Shield **18**

2.5.1. Shied Requirements 18

2.5.2. Description of the shield available 19

CHAPTER THREE: DETERMINATION OF DISINTEGRATION RATES 20

3.1. INTRODUCTION 20

3.2. THE DETERMINATION OF ACCURATE DEAD TIME PER COUNTING EVENT 20

3.2.1. Introduction 20

3.2.2. The Dead Time 20

3.2.3. Theoretical Considerations And Procedure 22

.

3.3. THE ACCURATE EFFICIENCY CALIBRATION 25

3.3.1. Introduction 25

3.3.2. Efficiency Calibration 25

3.3.3. Sources of Inaccuracies In The Measurements 26

3.3.4. Determination Of Measured Intensity 26

3.3.4.1. Background Correction 26

3.3.4.2. Decay during counting Correction 27

3.3.4.3. Dead time and pile-up Correction 29

3.3.4.4. True Coincidence Summing (TCS) Correction 32

3.3.4.5. Source Self Absorption Correction 33

3.3.4.6. Photon Attenuation Correction 33

3.3.5. The Efficiency Determination 33

3.4. The Disintegration Rate Determination **34**

3.5. Computer Programs **35**

3.5.1. Introduction 35

3.5.2. Calculations of the Measured Energy-Efficiency Data with NASEFFICAL 36

3.5.3. Linear Regression With Uncertainty From Both Coordinates (NASLINREG) 37

3.5.4. Fitting A Polynomial Function To The Energy-Efficiency Data (NASFIT). 38

3.5.5. Activity calculation with (NasActCal) 39

CHAPTER FOUR: EXPERIMENTAL SETTINGS AND RESULT **40**

4.1 INTRODUCTION **40**

4.2 THE SPECTROMETER SET-UP **40**

4.2.1 Initial Adjustments 40

4.2.2 Counting Geometry 41

4.2.3 Energy Calibration 44

4.3 Spectral Acquisition and Analysis **44**

4.3.1 Introduction 44

4.3.2 Determination of Full Energy Peak Areas using BACKGROUND STRIP METHOD 44

4.4 Efficiency Calibration **45**

4.4.1 Dead time per counting event 45

4.4.2 Measured Energy-Efficiency Data 46

4.4.3 Analytical Function Generation (Theoretical Model) 46

4.4.4 The Calibration Result 47

4.5 Determined Disintegration rates of Test Sources **49**

4.5.1 Introduction 49

4.5.2 The Disintegration Rate Determination Result 50

.

CHAPTER FIVE: SUMMARY, CONCLUSION AND RECOMMENDATIONS **52**

REFERENCES **54**

APPENDICES **57**

LIST OF TABLES

Table	Page
Table 4.1: Table presenting the result of determined activity of an Old ^{137}Cs source	50
Table 4.2: Table presenting the result of determined activity of an Old ^{60}Co source	51
Table III: Table of values showing the variation of the natural logarithm of the peak area A with increased total spectral count-rate R	64

LIST OF FIGURES

Figure Page

Figure 4.1: A plot of count-rate versus voltage for the detections system 43

Figure 4.2: Variation of Solid Angle with Source-Detector distances 43

Figure 4.3: The cross section of the Source-Detector geometry established 43

Figure 4.4**:** The plot of natural logarithm of the peak area A with increased total spectral count-rate R as scattered while the smoothed is the fitted equation, whose coefficient where found 46

Figure 4.5: The plots of the measured energy-efficiency data in comparison with the energy-efficiency function at various geometry levels 49

LIST OF APPENDICES

Table	Page
APPENDIX I: Fitting NaI Efficiency Calibration Data With Aksoy's (1993) Equation	57
APPENDIX II: Details Of Spectrometre Components Specifications	61

APPENDIX III: Table for the Moving Source Experimental Result

64

CHAPTER ONE

INTRODUCTION

1.1 Introduction

The activity of a radioactive source is its rate of disintegration. The determination of a source's disintegration rate can either be by the relative method (comparison with a known standard) or direct/ non –relative method. The use of relative method is simple but requires standard reference materials, with a large number of samples to be counted along. The standards serve the purpose of canceling the effect of the detector efficiency factor, which varies with the energies of the gamma photons and the counting geometry. The direct method of measuring a source disintegration rate can be by detecting and measuring all radiations from the source (4π-counting) or by detecting and measuring some of the radiation from the source under well known counting geometry and calibration e.g. the well defined solid angle counts method. In this work, a NaI(Tl) gamma ray spectrometer was set up and calibrated for activity measurements. This involved fixing of the counting geometry and the determination of the energy-efficiency relation.

The determination of the energy-efficiency relation can be achieved in so many ways like non-conventional (Gunnink, 1991), purely theoretical ways like Monte Carlo, Semi-experimental (use of detector specifications) like Zero Point Method (Gunnink, 1990), but the most reliable and accurate is the use of standard calibration sources (Debertin 1988).

Disintegration rate determination should always be finished with an uncertainty estimate. The factors contributing to the uncertainty may be due to systematic errors (experimental imperfections) or random errors (statistical). Systematic errors must be eliminated while random error must be minimized.

The inaccuracy in the determination of disintegration rate may be due to;

1. The statistics of the counts under an energy peak, which is the major uncertainty source in all low level measurements.
2. The Source-to-detector geometry (its variation in calibration source and real sample)
3. Coincidence summing
4. Dead time and pile up
5. Photon attenuation

If a correction factor cannot be obtained for any of these sources of inaccuracy from experiments, they should at least be estimated, and the estimates should be included in the total uncertainty. (Debertin 1998)

The International Atomic Energy Agency (IAEA) stresses the above fact as part of Quality Assurance (QA) and Quality Management in conducting analyses. In a technical document (IAEA-TECDOC-619), “Quality aspect of research reactor operations for instrumental neutron activation analysis” a Report of an Advisory Group meeting held in

Accra, Ghana, 18 –22 October 1999, under section 4.4 (*Conduct of analysis*) the above listed factors and more are outlined to assure the quality of analysed result (IAEA, 2001).

In order to comply with the International Quality Assurance (QA) standard, this project looked at the IAEA document, in an effort to establish Quality System for the analyses in CERT, as the main use of the Nigeria Nuclear Research Reactor NIRR-1 is for Instrumental Neutron Activation Analysis (INAA). NaI(Tl) spectrometer was used, alternate to HPGe, due to its efficiency and non requirement of Liquid Nitrogen, whose availability was a problem. A document on techniques in gamma spectroscopy using NaI scintillation detector as explored by " Gamma Ray Spectroscopy, Experiment GA, January 15, 2004" was also used as an additional guide.

The quality assurance factors listed by the IAEA (IAEA, 2001), and the measures taken to ensure compliance are listed below:

1 Synchronization of Clocks: The computer time was adjusted in comparison with GMT, and sources reference time well checked. The standard sources used for energy calibration reference time is in PST eight hours behind GMT.

2 Sample and Standard Physical dimensions: This apply to comparative INAA.

3 Ill-defined geometry of samples and/or standard: The project designed and constructed a sample holder to establish a well-defined (reproducible) geometry for standard sourced and samples.

4 Dead time effects: This was taken care of, by using the moving source methodology improved in the course of this project, to arrive at the dead time per counting event of the system.

5 Variable count rate during counting: In the methodology (chapter three of this thesis), Source decay during counting was corrected for analytically.

6 Pile up corrections: The method of dead time correction in (4) above incorporates pile up effect.

7 Coincidence or cascade summing effects: The calibrations in this project are at far geometry, region where this effect is negligible. Therefore, for subsequent measurements, this effect will also be negligible.

8 Gamma ray self-absorption effects: Standard point sources were used throughout this work. Hence, the effect is not applicable.

9 Background, shielding and contamination: Background spectra are used for residual background subtraction as the first correction (section 3.3.4.1), while the counting is done in a shield and all sources are sealed.

10 Exchange of samples: The samples involved were well labeled standard sources.

After this introductory chapter, chapter two reviewed some theories governing the spectrometer operation and related components, while chapter three outlined the methodology used in conducting this work. In chapter four we reported the experimental settings and result of various experiments and calculations performed and finally chapter five contains summary, conclusion and recommendations.

1.2 Literature Review

The deficiency of most of the works carried out in this area is lack of definite uncertainty (accuracy). Although Debertin et al (1976) calibrated Ge(Li) and HPGe detectors over a wide range emphasizing on accuracies, while they achieved activity determination using Sophisticated $4\pi\beta(X)$-γ coincidence method. A project conducted at Imperial College London (Usman, K., 2000) is the most relevant work studied and strictly adhered to, in the course of this project.

There are some other relevant works that were found useful such as the Ghanaian's work that calibrated N-type HPGe detector using an extended mixed standard radio-nuclide solution (Osae, et al 1999). At CERT, Jonah et al described some calibration points by efficiency function containing four fitting parameters for a NaI detector (Jonah, 2000). Monte Carlo method was used to determine Full Energy Photo-peak Efficiency (FEPE) for a HPGe by another CERT staff at Budapest (Ewa, et al 2001). Conventional methods that use detector specifications and few sources to arrive at the FEPE function (Gunnink, 1991) or even without a source called Zero Point Method (Gunnink, 1990) were studied, but they are unique to HPGe detector. Finally a very useful work conducted at Energy Research Laboratory Institute of The King Fahd University of Petroleum and Minerals, Dhahran, Saudi Arabia (Aksoy 1993), provided a mathematical model of FEPE functions developed for an HPGe spectrometer. This work tested the model among others and found it the best that fits the NaI(Tl) spectrometer used.

1.3 Justification

Nigeria has commissioned its first Nuclear Research Reactor (NIRR-1), a Miniature Neutron Source Reactor (MNSR) type. The facility will be used for various research purposes.

Mainly the MNSR will be used for Neutron Activation Analysis (NAA). This involves irradiation of sample with the reactor, which later emits characteristic gamma rays, which are the signatures of the elements in the samples. The measurement of the emitted gamma rays, require a well-calibrated gamma ray spectrometer.

The work is all about the proper setup and calibration of a NaI(Tl) gamma ray spectrometer that will serve as an alternative or a compliment to the HPGe gamma ray spectrometer use for measurements at MNSR facility .

1.4 Objective

The aim of the project is to properly setup and calibrate NaI(Tl) gamma ray spectrometer for accurate measurement of source disintegration rates. This was achieved through; setting up the spectrometer, conducting energy and efficiency calibrations as well as simplifying the associated calculations to arrive at definite energy-efficiency function for the spectrometer. The knowledge of this function is the major requirement in determining source disintegration rates without using any standard reference material.

CHAPTER TWO

GAMMA SPECTROMETRY AND THE SPECTROMETRE COMPONENTS

2.6. Introduction

This chapter explores the theory behind radiation detection; the basic interactions involved, detector types and the operational principle of Inorganic Scintillation detectors a group to which the NaI(Tl) detector used in this work belongs. The specifications of all the spectrometer components and the description of the available shield are also included.

2.7. Interactions of Gamma Radiation with Matter

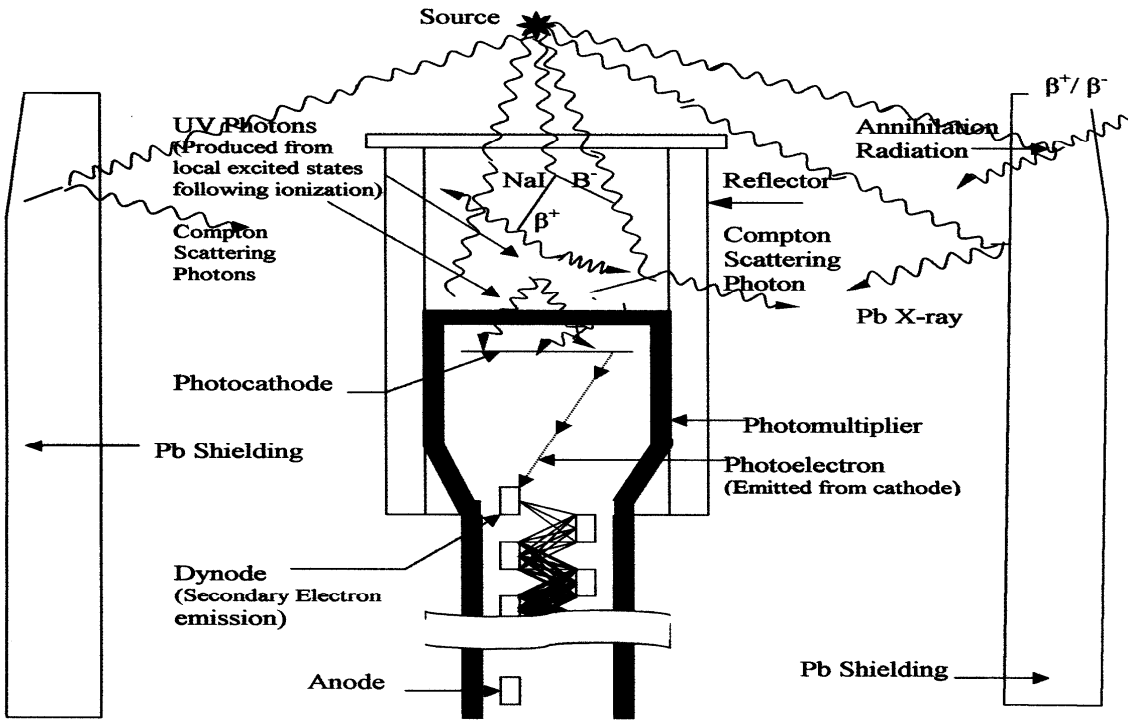


Figure 3: A Schematic of a NaI (Tl) detector and a source showing various gamma ray interactions

Gamma photon interaction with matter (Atoms) can occur in numerous ways, but the three most significant ones are: Photoelectric absorption, Compton scattering and Pair production. In all these three interactions the photon along its track in the matter loses

energy totally or partially, leading to the production of electrons (electron-ion or electron-hole pair), thereby changing the photon history. This is what detectors use to detect passage or determine energy of photon by measuring the quantity of charges (electrons) produced. We shall describe each one of these briefly.

2.7.1.Photoelectric Absorption

In this interaction all the photon energy is transferred to a bound electron as its kinetic energy, minus the energy used in releasing it (binding energy). Eighty percent of the photoelectric interactions occur in K-shell (most tightly bound), and it is the predominant mode of interaction at low photon energy, from Debertin and Helmer (Debertin, 1988) its energy given by:

$$E_e = E_\gamma - E_b \qquad (2.1)$$

where;

E_e – is the energy of electron ejected from the atom

E_b – is the binding energy of electron ejected from the atom

E_γ – is the energy of the photon

In most cases the photon energy is absorbed near the interaction site, as the hole left by the ejected electron is filled by rearrangement of other shells' electrons or capture of free electrons, this leads to emission of X-ray or Auger electrons. In this way the excitation energy of the atom is carried away.

The interaction probability (τ) depends on the photon energy and the atomic number Z of the absorbing material. Based on this the detector and shielding materials are chosen. This relation is not defined but the following equation is commonly used from Debertin and Helmer (Debertin, 1988):

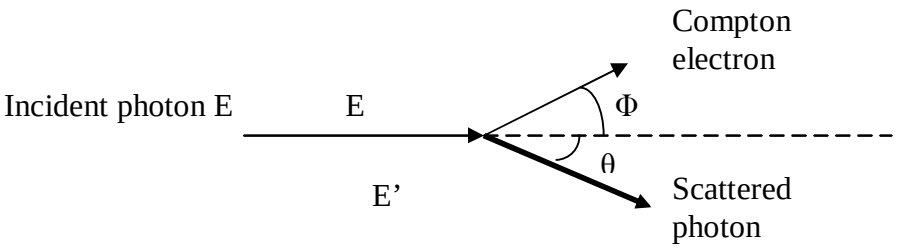
$$\tau = const \cdot Z^{4.5} \cdot E_{\gamma}^{-3} \quad \text{——————} \quad (2.2)$$

The plot of photoelectric absorption cross-section for a popular gamma ray detection material NaI can be found in Figure 2-18 of Knoll G. F., which shows the K-edge around 0.033 MeV (33KeV), the threshold energy value for photoelectric interaction to occur. This is good compared to much higher Z elements like Germanium and Silicon, where the K-edge is around 10.5 KeV and 2.4 KeV respectively as found by Storm and Israel 1970 (Debertin 1988).

2.7.2.Compton Scattering

This is frequently the predominant interaction mechanism for gamma ray energies for typical radioisotope sources. The energy range is between 50 KeV to 10 MeV.

In this interaction an incident photon comes in contact with an absorber electron assumed to be at rest, and is deviated from its path through a scattering angle θ, which results in less energetic secondary photon and a recoil electron. The sum of the energies of the secondary photon and a recoil electron should be equal to that of the incident photon by conservation of momentum. How they share the incident photon energy is determine by θ, which can take any value, and are related as follows (Knoll, 1979):



If $\alpha \equiv h\nu / m_o c^2$

The energy of the secondary photon is

$$E' = E[1 + \alpha(1 - \cos\theta)]^{-1} \quad \text{——————} \quad (2.3)$$

while the energy of the scattered electron is

$$E_e = E.\{1 - 1/[1 + \alpha(1 - \cos\theta)]\} \quad \text{——————} \quad (2.4)$$

The two angles are related by

$$\tan\Phi = 1/[1 + \alpha.\tan(\theta/2)] \quad \text{——————} \quad (2.5)$$

The interaction here is not localized, but spread over the absorber as the secondary photon continues to scatter before finally vanishing through photoelectric effect. To account for this the track of all the subsequent photons has to be followed. This necessitates the knowledge of the probability that a photon will scatter.

Scattering probability is given by Klein-Nishina formula in differential cross-section form

$$\frac{d\sigma}{d\Omega} = r_0^2\left[\frac{1}{1+\alpha(1-\cos\theta)}\right]^3\left[\frac{1+\cos^2\theta}{2}\right]\left[1+\frac{\alpha^2(1-\cos\theta)^2}{(1+\cos^2\theta)[1+\alpha(1-\cos\theta)]}\right] \quad \text{——————} \quad (2.6)$$

The graphical representation of this relation, is given in (Debertin 1988) and (Knoll 1979). They all associate its dominance to higher gamma ray energies.

The Compton scattering absorption cross section is also related to the energy of gamma ray in practical gamma ray book (Gilmore, 1995) by the relation below;

$$\sigma \propto 1/E_{\gamma} \qquad \text{(2.7)}$$

2.7.3.Pair Production

This is the leading interaction mechanism for gamma rays in the order of few MeV. The photon disappears and is converted to positron-electron pair within a nuclear Coulomb field. 1.022 MeV is the threshold for pair production. Conservation of momentum must also be satisfied. It is achieved through an inverse process called annihilation, in which a particle and its antiparticle collide to annihilate each other, the total energy of the two particles appearing as electromagnetic radiation. This occurs in solid, which provides the electrons needed. The momentum after annihilation must be almost zero, and this can only happen if the two photons are emitted in opposite direction to cancel their momenta.

2.8. Radiation Detectors

There are various types of gamma radiation detectors, the most commonly used include

I. Gas-Filled Detectors:

There are three major ones; Ionization Chambers, Proportional Counters and Geiger-Mueller Counters

II. Scintillation Counters:

They are basically of two types; Organic Scintillators and In-*o*rganic Scintillators, they are coupled with Photomultiplier Tubes. These will be further explained in the next section, when the NaI (Tl) used in this work is discussed.

III Semiconductor Detectors:

They are of three groups; Semiconductor Diode Detectors, Lithium Drifted Germanium Detectors and High Purity Germanium (HPGe). There exist Other Solid state Detectors as well (knoll 1979).

2.8.1. Scintillation Detectors

Scintillation detection is base a certain property of some materials that emit light when in contact with ionizing radiation. This process is known as fluorescence. Ideally such materials should posses the following properties (knoll, 1979):

1. They should convert the kinetic energy of ionizing radiation into detectable light with high scintillation efficiency.
2. Their light yield should be proportional to deposited energy over a wide possible range.
3. Their media should be transparent to their respective emission wavelength, for good light collection

4. The decay time of the induced luminescence should be short to ensure fast signal generation
5. They should be of good optical quality and subject to manufacture in sizes large enough to be of interest as practical detector.
6. Their refractive index should be close to that of glass to permit efficient coupling of the scintillation light to Photomultiplier tube.

   The most favorable and closest to this ideality practically is sodium iodide (NaI) Crystal.

When light emission from the materials follows excitation immediately, it is termed Prompt fluorescence, if slower and having longer wavelength it is termed phosphorescence and there can be delayed fluorescence when the characteristic time is much slower. A good scintillator maximizes the first and minimizes the rest.

Scintillators are classified into two major categories namely Organic and Inorganic. Organic Scintillators are much faster, but the light yield is low. They have low atomic number (Z) compared to Inorganic ones, which make them suitable for beta and fast neutron detection, whereas Inorganic Scintillators suit gamma spectroscopy better. Therefore in this project we shall concentrate on Inorganic Scintillators.

2.8.2. Inorganic Scintillators

The crystal lattice of an inorganic material determines its energy state. Excitation causes the valence band electron to move towards conduction band leaving a hole behind.

In pure crystal, it returns immediately by emitting photon, which is invisible due to the speed of the process. To obtain visible photons, activators are introduced into the crystal. They create additional energy levels in the forbidden gap of the pure crystal, which allows excitation from valence band to an activator's (excitation) energy level and return to its ground state (not valence band). This process makes the emitted photon visible. This is how Scintillation occurs.

Electron-hole pairs are created by incoming charge (radiation) as it excites electrons from valence band. The activator causes drift of the holes toward itself to get ionized, since it has lower ionization energy than the crystal while the electron moves around until it meets an ionized activator. If it lands in an allowed excited (activator) state, and de-excites quickly it emits a visible photon. It is important to note that *Phosphorescence* and electron capture compete with the above phenomenon to cause delay and *quenching* (no Photon) respectively. If the electron–hole pair move in loose associate manner till they meet the activator the process is called *exciton*, while light is released in as earlier mentioned.

The existing Inorganic Scintillators are basically made of Alkali Halide (e.g. NaI(Tl), CsI(Tl), CsI(Na) and LiI(Eu)), Glasses (containing Lithium), Gases (e.g. Xenon and Helium) and other Miscellaneous (Inorganic compounds e.g. ZnS(Ag), CsF, CAF2(Eu) and Bismuth Germanate)). Amongst all the inorganic Scintillators mentioned above, NaI(Tl) is of major interest here.

2.8.3. NaI (Tl) Detector

Sodium iodide NaI (Tl) is noted for excellent light yield, being the highest among all scintillation materials. Its response to gamma rays (and electrons) is almost linear. It is also accepted as the standard Scintillation material for routine gamma ray spectroscopy. It can be shaped easily, even thought the crystal is fragile and hygroscopic (knoll, 1979).

2.8.4. Photomultiplier Tubes

Photomultiplier Tubes convert weak light output of a scintillation pulse into a corresponding electrical signal, without adding large amount of noise to it. They consist mainly of photosensitive layer called *photocathode,* coupled to an electron multiplier structure, which converts the incident photons into low energy electrons called *photoelectrons*. These photoelectrons are too small in number to be detected as electrical signal. They are collected and further amplified linearly by the electron multiplier section, which produce detectable signal at the anode.

2.9. Description of the Spectrometer Components

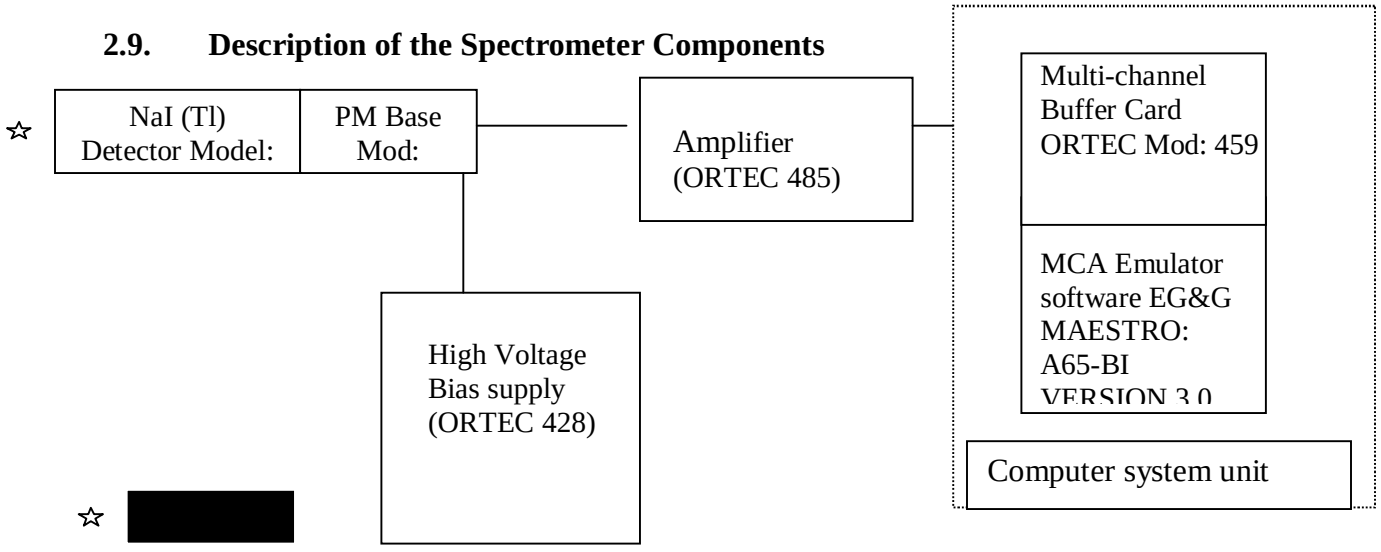


Figure 1: The Block diagram for NaI (Tl) Gamma-Ray Spectrometer

2.9.1. Characteristics of the NaI (Tl) Detector used

The following is extracted from CANBERRA CATALOG and the detector body.

The detector under consideration is a NaI (Tl) type, made in USA by CANBERRA. Each NaI (Tl) is enclosed in a chrome-plated aluminum housing, for easy cleaning of contaminants. Chrome plated metal is the light shield around the Photomultiplier tube to minimize gain changes due to nearby electric motors and earth's magnetic field.

Description;

Model Number: Model 802-4

Serial Number: 8904425

The detail of its specification is in Appendix II.

2.9.2. The Photo Multiplier Tube And Preamplifier

The Photomultiplier is PM Tube Base – Preamplifier, also from CANBERRA CATALOG and from its body, the following were extracted.

Model Number: Model 2007P

Serial Number: 12903791

The details of its specification are given in Appendix II.

2.9.3. The Minibin And Power Supply

The minibin on which sits the modules, contains and ORTEC 402A power supply, having Serial Number: 13279.

This minibin enables various standard nuclear modules to be mounted and moved easily. On it modules are connected among which is the power supply, detector bias supply and amplifier. The details of its specification are given in Appendix II.

2.9.4. The Detector Bias Supply

The power supply is a double width NIM (Nuclear Instrument Module) module, It is an EG &G ORTEC Model 428, which provides bias voltage of either polarity (Positive used). The outputs are short-circuit proof with an impedance of approximately 1.3MΩ, and each has a range of 0 – 1000 V. These output are selected independently by 10-turn direct reading potentiometers. Some high-grade circuits with <0.0002% noise and ripple, supply constant bias voltage. The details of its specification are in Appendix II.

2.9.5. The Linear Amplifier

The amplifier is a single width NIM module, EG&G ORTEC, model 485 spectroscopy amplifier with variable pole-zero cancellation and an active filter. Its specification is in Appendix II.

2.9.6. The Computer System Unit

This unit comprises of a computer system (EG&G ORTEC) with Multi-Channel Buffer card attached and Multi-Channel Analyzer (MCA) Emulator software (EG&G MAESTRO.

The EG & G ORTEC Model 459 Multi-Channel Buffer card makes the computer to serve as controlled Multi-Channel pulse height analyzer, and it is a single slot Peripheral Component Interconnect (PCI) card.

The associated acquisition software is MAESTRO, Model: A65-BI VERSION 3.0 Emulation software, [MCB_CTRL_DLL 3.20] [MCB C10_DLL 2.31].

2.10. The Shield

2.10.1. Shield Requirements

To reduce the background gamma radiation reaching the detector from the surrounding, a shield is required. In this work, an annular lead shield, which was available in the centre was used.

However the general shield design considerations are (Gilmore 1995):

1. High density material with low mass attenuation coefficient
2. Large inner diameter for detector to be far from gamma ray resulting from the shield
3. Iron could be used, because it is cheap, however Cobalt contamination, in addition to gamma backscatter make it disadvantageous.

Thus Lead is better because Compton scattering is less inside and more the following characteristics are to be considered:

a. Optimum limit of thickness due to cosmic interaction is (100-150) mm
b. It has the problem of releasing lead fluorescent X-ray peaks into the gamma spectrum

This problem can be averted by absorption from lighter elements like Cadmium, Tin or Copper, but cadmium also generate X-rays which 0.7mm of Cu can absorb. In neutron environment (like ours) Cadmium should be avoided due to its high neutron affinity and its toxic when subjected to heat.

2.10.2. Description of the shield available

The shield is a cylindrical hollow case opened both at the top and bottom to allow the insertion of the sample holder and the detector, respectively. The internal diameter is around 11cm, which is not so sufficient to keep the detector away from the radiation resulting from the shield, compared to 50cm of the reactor hall shield.

The wall is made from inner layer to outer layer with tin, stainless steel, copper, the major material Lead and then another stainless steel respectively. They are all encased with a handle made of metal, for easy mobility.

The major material used is an old lead (pre-1950s recommended), supported by tin and copper to absorb the fluorescence-ray, and lastly stainless steel to reduce bremsstrahlung.

A table showing the thickness of the set up is in Appendix II.

CHAPTER THREE

DETERMINATION OF DISINTEGRATION RATES

3.1. INTRODUCTION

The method for the determination of measured gamma ray intensity requires the knowledge of accurate efficiency as an analytical function of energy. This chapter explains how the dead time of the NaI(Tl) spectrometer was determined and how the efficiency Calibration was done and used to accurately determine gamma ray intensities, which are converted to the disintegration rate or activity of a source.

3.2. THE DETERMINATION OF ACCURATE DEAD TIME PER COUNTING EVENT

3.2.1. Introduction

In this work, the method of dead time determination known as "Moving Source" Method (Gilmore, 1995), was adapted, modified and optimized.

3.2.2. The Dead Time

The dead time of a spectrometer refers to the time it takes the spectrometer to process a single signal. During that period it cannot register another signal. It is then said to be dead. The knowledge of this time is very important in assuring the quality of gamma spectroscopy. The knowledge of the dead time is needed to correct for the count loss during the period.

There are two basic types of dead times: the paralyzable (extending) and non-paralyzable (non-extending). All photon-counting systems can be described by one of these two types, or by a combination of these two types (Jenkins et al, 1981). To a single isolated photon both respond in the same way, but to two successive photons, the arrival of the second photon in non-paralyzable is ignored, while in paralyzable extends the dead time. In this work we used non-paralyzable model.

The dead time of gamma spectrometers, arise from the electronics, especially the linear amplifier. The dead time will therefore be of the order of the shaping time of the linear amplifier, that is few microseconds, but it is always better determined experimentally (Gilmore, 1995).

There are various practical dead time correction methods that can be employed to determine dead time such as: Manual, Philips, Simple Live clock, Lowes' Live time,

Gedcke-Hale Live time clock, Harms', Barnhart and the Moving Source methods (Jenkins et al, 1981). The moving source method is chosen because it is the one recommended by the quality assurance document of the International Atomic Energy Agency (IAEA) TEC-DOC-1218 (IAEA, 2001). Its advantage is that one can correct for the dead time and pile-up simultaneously without leaving pile-up residue (Gilmore, 1995), especially in this case where the linear amplifier does not have pileup rejection circuit.

A major source of dead time which most of the methods do not take into account is the pile-up; they usually rely on the pile-up rejection circuits. Even with pile-up rejection circuit there must be some residual random coincidences. There is then, whether or not pile-up rejection is available, a need to be able to correct for random summing especially in high count-rates (Gilmore, 1995).

To accurately determine the dead time, a recent method of finding uncertainty in slope and intercept which unified the equations for the slope, intercept, and standard errors of the best straight line (York and Evensen, 2004) was programmed in this work (Section 3.3.2) using Visual Basic 5.0, where both the coordinate axes under consideration have their respective uncertainties.

The Moving Source experimental procedure has been improved and used along with the unified equations for the slope, intercept, and standard errors of the best straight line to determine the dead time and its uncertainty. Uncertainties have been analysed and propagated throughout the work respectively (Taylor, 1997)

3.2.3. Theoretical Considerations and Measurement Procedure

A gamma photon will be involved in a summing whenever it is not preceded by a certain definite period of time. The derivation below is from a practical gamma ray book (Gilmore,1995):

Let τ, be the resolution time of the electronic system.

According to Poisson distribution it can be shown that the probability of a random coincidence, P, within τ is

Where R is the mean count rate

$$P = 1 - \exp(-2R\tau) \qquad (3.2.1)$$

The fractional loss in the peak area due to this random summing (pile-up) effect is.

$$\frac{(A_T - A)}{A_T} \qquad (3.2.2))$$

~~P A is the measured peak area and A_T is the true peak area.~~

By definition of probability the above two equations (3.2.1) and (3.2.2) are the same.

Therefore;

$$\frac{(A_T - A)}{A_T} = 1 - \exp(-2R\tau) \qquad (3.2.3)$$

Re arranging equation (3.2.3) above gives;

$$A_T = A \exp(2R\tau) \qquad (3.2.4)$$

This equation (3.2.4) is the expression for the true count required. To solve for the true count, the mean count-rate and the resolution time, τ, are needed. If there is no pile-up effect, it can be taken to be the same as the shaping time constant of the amplifier. It is best estimated by experiment.

Taking logarithm of equation (3.2.4), after re-arranging yields;

$$\ln(A) = \ln(A_{true}) - 2R\tau \qquad (3.2.5)$$

Since equation (3.2.5) is linear, hence a plot of ln(A) versus the count-rate, R, a straight line with slope 2τ, from where, τ, can be found.

To find the count rate R, one could use a count-rate metre, which would have its own different pile-up problems. Practically, the easiest way is to measure the count-rate within the spectrum itself, which is the summation of all counts in the spectrum, divided by the live-time. R will not be absolutely accurate because pulses below the lower threshold of the ADC and those outside the linear gate window will not be taken into account. Nevertheless, the method provides a convenient measure of count rate sufficient to provide an empirical estimate for the system's resolution time (Gilmore, 1995).

Considering the above theory, both the peak area A and the total count-rate R have uncertainties, which have to be propagated in order to obtain the uncertainties in the slope and the dead time, τ.

The steps involved in the conduct of the experiment are outlined below:

1. Cs-137 source was fixed in a position near the detector that a total count-rate of 2000cps was obtained. It was then left there throughout the experiment.
2. Three Spectra were accumulated for some time in an effort to obtain the peak area for the 661.6 KeV peak of the Cs-137, with a precision of less than one percent.
3. The area under Cs-137 (661.6 KeV) peak was measured and the mean count-rate calculated.
4. Eu-152 source (IAEA recommended as it resembles NAA Spectrum) was introduced into the spectrum, in order to enable variation in the count-rate of the spectrum.
5. The spectrum was measured and step three (3) repeated.
6. The Eu-137 source was moved closer to the detector so as to increase the count-rate and the measurement was repeated.

7. Step six (6) was repeated seven more times (as allowed by the geometry), until the Eu-137 source was very close to the detector.
8. A graph of ln(*A*) against the count-rate *R* was plotted with Microsoft excel spread sheet for visualization.
9. The designed program was used to calculate the slope of the graph of ln(*A*) against the count-rate *R* as well as its uncertainty.
10. The experiment was performed three times to optimize the counting time, in such a way that the uncertainty level is acceptable for use in subsequent gamma ray spectroscopy works/calculations.

3.3. THE ACCURATE EFFICIENCY CALIBRATION

3.3.1. Introduction

A gamma ray spectrometer measures the energy and intensity of gamma radiation. This measurement involves the determination of the Full-Energy-Peak-Efficiency (FEPE) as a function of photon energy (Debertin 1988). This section explains how FEPE was measured using point standard sources and the mathematical function fitted to the data for subsequent interpolation.

3.3.2. Efficiency Calibration

Generally, for single photon energy (peak) its measured gamma-ray intensity (I) is given by;

$$I = \frac{c}{T} f_1 f_2 f_3 \ldots \qquad (3.2.0)$$

where C is the measured count in a peak

T is counting (live) time of measurement

f_i are the correction factors

(Debertin 1988)

3.3.3. Sources of Inaccuracies In The Measurements

The correction factors in equation (3.3.0) that were considered in order to improve the accuracy of the measurement result are as follows:

1. Background
2. Source decay during counting
3. Dead time and pile-up
4. True Coincidence Summing
5. Source self-absorption
6. Photon attenuation

This project minimized (1) and (4) physically, corrected for (1), (2) and (3) analytically, while (5) and (6) were considered negligible in this respect.

These factors are discussed in the next section.

3.3.4. Determination Of Measured Intensity

3.3.4.1. Background Correction

The background radiation results from other radioactive materials present within the vicinity of the detector, such as wall (paint), appliances or even other radiation sources.

The lead shield minimizes the background radiation, by attenuating the photons, as they tend to reach the detector. The residual background within the detector-shield space is further subtracted from the peak count, through the acquisition of separate spectra (background spectra).

The corrected count (C) is given by

$$C = C' - C_b \qquad (3.3.1)$$

with uncertainty

$$\sigma_C = \sqrt{\sigma_{C'}^2 + \sigma_{Cb}^2} \qquad (3.3.2)$$

where C' is raw counts under the peak

C_b is the background count under same channel as (C')

σ_i signifies uncertainty in i

This background strip was used to achieve background subtraction, using the MAESTRO acquisition software.

3.3.4.2. Decay during counting Correction

A radioactive source decays continuously, even as it is counted especially when the counting time is long compared to its half-life. This was corrected for analytically, the derivation is from the Ph. D thesis (Usman, 2000):

The corrected count is the continuous summation of the gamma ray intensity ($I_{\gamma C}(t)$) over time t, written mathematically as;

$$C = \int_o^t I_{\gamma C}(t)\, dt \qquad (3.3.3)$$

When the above equation is taken with respect to the time at the beginning of counting (t_b) then;

$$C = \int_o^{t_c} I_\gamma(t_b)\, e^{-\lambda t}\, dt \qquad (3.3.4)$$

$$I_\gamma(t_b) = \frac{I_{\gamma C}\, t_c\, \lambda}{(1 - e^{-\lambda t_c})} \qquad (3.3.5)$$

where: $I_{\gamma C}$ is the measured intensity

t_c is the counting time

λ is the decay constant

Which can be rearranged as:

$$I_{\gamma}(t_b) = \frac{C\ \lambda}{(1 - e^{-\lambda t_c})} \qquad (3.3.6)$$

$$I_{\gamma}(t_b) = \frac{C\ \ln 2}{T_{1/2}\left(1 - e^{-\frac{tc\ \ln 2}{T_{1/2}}}\right)} = \frac{I_{\gamma C}\, t_c\ \ln 2}{T_{1/2}\left(1 - e^{-\frac{tc\ \ln 2}{T_{1/2}}}\right)} \qquad (3.3.7)$$

with associated uncertainty obtainable from;

$$\sigma^2_{I\gamma}(t_b) = \left(\frac{\partial I_{\gamma}(t_b)}{\partial C}\right)^2 \sigma^2_c + \left(\frac{\partial I_{\gamma}(t_b)}{\partial T_{1/2}}\right)^2 \sigma^2_{T_{1/2}} \qquad (3.3.8)$$

This becomes:

$$\sigma^2_{I\gamma}(t_b) = I_{\gamma}(t_b)\left[\left(\frac{\sigma_c}{C}\right)^2 + \left(1 - \frac{t_c e^{-\lambda t_c}\ \ln 2}{T^2_{1/2}(1 - e^{-\lambda t_c})}\right)^2 \sigma^2_{T_{1/2}}\right]^{1/2} \qquad (3.3.9)$$

3.3.4.3.Dead time and pile-up Correction

The details have been discussed earlier in section (3.2) of this thesis. The two are treated as one, because many of the automatic dead-time correctors in energy dispersive spectrometers are based on ideal live-time clock, which provides exact compensation for the loss of pulses that arrive during the time the system is processing a previous pulse. Unfortunately, the simple live-time clock does not compensate for the loss of a preceding pulse when another pulse arrives, before the height of the first pulse can be measured without pile –up distortion (Jenkins et al, 1981).

If the measurement live time is used in the determination of the count rate as counting time t_c, dead time is taken care of by the live time clock of the acquisition software (Debertin 1988), but pile-up rejection has to be considered and corrected seperately.

The pile up can be corrected by the electronic pile-up rejection system, but there still remain residual random coincidences especially in high count rate (larger than $1000S^{-1}$ according to Debertin (1988)) spectra (Gilmore 1995).
This can be accomplished through moving source experiment as suggested by Jenkins et al (1981), described by Gilmore, (1995) and Debertin, (1988), the results give the effective dead time (per count) in the system τ_d.

The moving source experiment is carried out, as described in section 3.2.
In any case where the empirical method of dead time correction is employed, as above, the intensity of the gamma ray at the beginning of counting is obtained as follows, the derivation is from the Ph. D thesis (Usman, 2000):
If the:
Dead time is τ_d
True count rate is N_t
Observed count rate is N_o

Fraction of the total dead time for which the system is dead is $N_o \tau_d$

This implies that the;

The rate of loss of pulse is $N_t N_o \tau_d$

Also the rate of loss of pulse is $N_t - N_o$

Therefore,

$$N_t - N_o = N_t N_o \tau_d \qquad (3.3.10)$$

hence

$$N_t = \frac{N_o}{1 - N_o \tau_d} \qquad (3.3.11)$$

But

$$C = \int_o^t I_\gamma (t)\, dt \qquad (3.3.12)$$

Combining the above two equations gives;

$$C = \int_o^{tc} \frac{I_\gamma (t_b) e^{-\lambda t}}{I + \tau_d I_\gamma (t_b) e^{-\lambda t}} dt \qquad (3.3.13)$$

$$C = \frac{1}{\lambda \tau_d} \ln \left(\frac{1 + \tau_d I_\gamma (t_b)}{1 + \tau_d I_\gamma (t_b) e^{-\lambda t}} \right) \qquad (3.3.14)$$

This implies that

$$I_\lambda (t_b) = \frac{1 - e^{-\lambda c \tau_d}}{\tau_d (e^{\lambda (c\tau_d - t_c)} - 1)} \qquad (3.3.15)$$

The uncertainty is propagated using

$$\sigma^2_{I\gamma(t_b)} = \left(\frac{\partial I_\gamma (t_b)}{\partial C} \right)^2 \sigma_c^2 + \left(\frac{\partial I_\gamma (t_b)}{\partial T_{1/2}} \right)^2 \sigma^2_{T_{1/2}} + \left(\frac{\partial I_\gamma (t_b)}{\partial \tau_d} \right)^2 \sigma^2_{\tau_d} \qquad (3.3.16)$$

Equation (3.3.16) when expanded and rearranged becomes

$$\sigma_{I_\gamma(t_b)} = I_\gamma(t_b)\left[\left[\frac{\lambda C\tau_d(1-e^{-\lambda t_c})e^{\lambda c\tau_d}}{e^{\lambda(c\tau_d - t_c)}-1}-1\right]^2\left(\frac{\sigma_{\tau_d}}{\tau_d}\right)^2+\left[\frac{\lambda C\tau_d(1-e^{-\lambda t_c})e^{\lambda c\tau_d}}{(e^{\lambda(c\tau_d - t_c)}-1)(1-e^{\lambda c\tau_d})}\right]^2\left(\frac{\sigma_c}{C}\right)^2 - \left[\frac{\lambda C\tau_d(1-e^{-\lambda t_c})e^{\lambda c\tau_d}+\lambda t_c(1-e^{\lambda c\tau_d})e^{\lambda(c\tau_d - t_c)}}{(e^{\lambda(c\tau_d - t_c)}-1)(1-e^{\lambda c\tau_d})}\right]^2\left(\frac{\sigma_{T_{1/2}}}{T_{1/2}}\right)^2\right]^{1/2}$$

(3.3.17)

3.3.4.4. True Coincidence Summing (TCS) Correction

This factor is also known as summation effect. This source of uncertainty comes as a result of summing of gamma rays emitted very nearly simultaneously from the nucleus. In other words it occurs with radionuclides that emit two or more gamma photons simultaneously, when this happens within the resolving time of the spectrometre, a sum pulse is recorded somewhere else, leading to count loss in the actual peak of those photons. (Debertin 1988)

TCS results in lower full-energy-peak areas. It worsens, as the source gets closer to the detector, with larger detectors or when the detector window is thin (i.e. cannot absorb x-rays). It is worst in well type detectors.

It can be expected whenever nuclides with complex decay scheme are measured, though the degree of summing is count-rate independent (Gilmore 1995). This fact was considered while establishing the source to detector geometry using equation (3.3.18) below;

$$\Omega = 2\pi\left(1 - \frac{d}{d^2 + r^2}\right) \qquad (3.3.18)$$

Where **Ω Is the Solid angle**

D is the source to detector distance

R is the radius of the detector

Far away from the detector, possibility of TCS is less hence its effect becomes negligible (Gilmore 1995). This is why this project narrowed down to far geometry. The project calibrated relatively far geometries.

3.3.4.5. Source Self Absorption Correction

This occurs in large volume source, where the source itself absorbs (attenuates) radiation from its inner part. The sources used, are standard point sources with very small volume, therefore this correction is negligible.

3.3.4.6. Photon Attenuation Correction

This occurs if there is any dense material, capable of changing (decreasing) the gamma ray intensity, in the space between a source and the detector. This correction should only be applied if the sources used for efficiency calibration and the sources under study differ in their photon attenuation properties (Debertin 1988).

The sources are enclosed in a light plastic casing, and the space between them and the detector Aluminum end cap is filled with still air, therefore this factor is negligible.

3.3.5. The Efficiency Determination

Having gotten the corrected measured intensity of the gamma ray Iγ at the beginning of counting (t_b) written as Iγ (t_b), the efficiency can be calculated using:

$$\varepsilon_\gamma = \frac{I_\gamma(t_b)}{P_\gamma I_s(t_s) Exp\left[-\ln 2\left(\frac{t_b - t_s}{T_{1/2}}\right)\right]} \qquad (3.3.19)$$

where

I_S (t_b)= quoted activity evaluated at manufacturer's reference time

P_γ = Emission probability of the gamma ray

ε_γ = Absolute photo peak efficiency

t_b = time at the beginning of counting

t_S = time of manufactures quoted activity

$T_{½}$ = Half life of the source

The above equation (3.3.19) has the following associated uncertainty:

$$\sigma_{\varepsilon\gamma} = \varepsilon_\gamma \left[\left(\frac{\sigma_{I\gamma(t_b)}}{I_\gamma(t_b)}\right)^2 + \left(\frac{\sigma_{p_\gamma}}{p_\gamma}\right)^2 + \left(\frac{\sigma_{I_s(t_s)}}{I_s(t_s)}\right)^2 + \frac{((t_b - t_s)\ln 2)^2}{T_{1/2}^2}\sigma_{T_{1/2}}^2\right]^{1/2} \qquad (3.3.20)$$

Evaluating equations (3.3.19) and (3.3.20) above, for each gamma energy peak from many standard sources, yields the measured energy-efficiency data. An analytical energy-efficiency function can then be fitted to the data to enable interpolation.

Arbitrary polynomials were fitted to the efficiency data (Aksoy 1993), using least square method, the polynomial degree was chosen based on least weighted mean deviation. The detail is in section (3.5.4).

3.4. The Disintegration Rate Determination

Carrying out the above operations (3.1 to 3.3) on a spectrometer fully sets it up for accurate measurement of gamma ray energies and intensities. Generally the activity is obtained from intensity by multiplying it by the gamma emission probability (P_γ). After obtaining the energy-efficiency function, the activity (at a reference time t_s before t_b) and its uncertainty for a source can be obtained from the measured intensity of the the gamma rays it emits using equation (3.3.19) when rearranged as shown below:

$$I_s(t_s) = \frac{I_\gamma(t_b)}{P_\gamma \varepsilon_\gamma Exp\left[-\ln 2\left(\frac{t_b - t_s}{T_{1/2}}\right)\right]} \qquad (3.3.21)$$

The propagated uncertainty is

$$\sigma_{I_s(t_s)} = I_s\left[\left(\frac{\sigma_{I\gamma(t_b)}}{I_\gamma(t_b)}\right)^2 + \left(\frac{\sigma_{p_\gamma}}{p_\gamma}\right)^2 + \left(\frac{\sigma_{\varepsilon_\gamma}}{\varepsilon_\gamma}\right)^2 + \frac{((t_b - t_s)\ln 2)^2}{T_{1/2}^2}\sigma_{T_{1/2}}^2\right]^{1/2} \qquad (3.3.10)$$

where, ε_γ is the interpolated efficiency and $\sigma_{\varepsilon\gamma}$ its uncertainty.

3.5. Computer Programs

3.5.1. Introduction

Obviously, using the equations in section (3.3) requires a computer program. This Section describes the programs written at various stages of the project, with the aid of some mathematical concepts obtained from Bevignton (1992), Frank (1994), Gupta (1993), Kreyszig (1993) and William (1992).

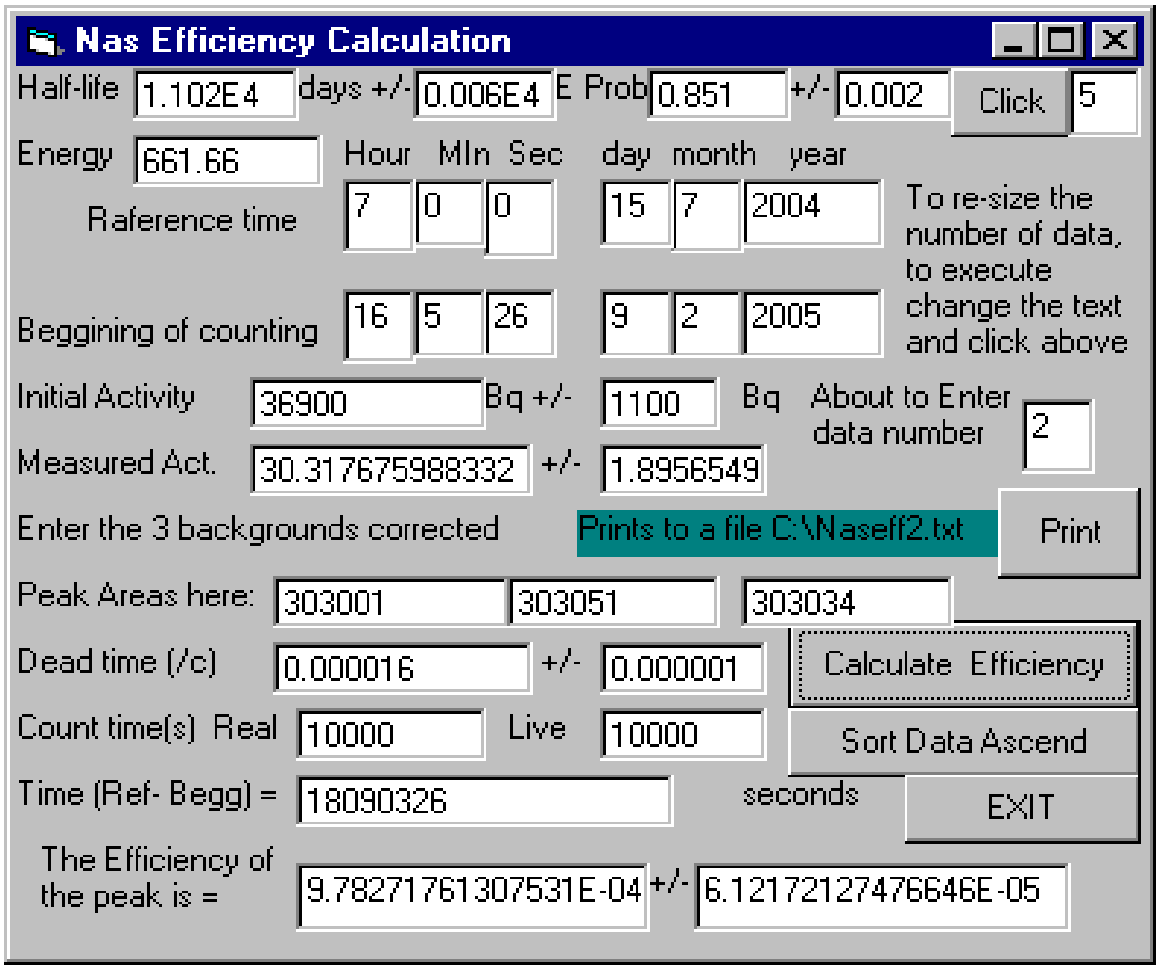
There are four programs written for various purposes namely:

1. NASEFFICAL
2. NASLINREG
3. NASFIT
4. NASACTCAL

We shall discuss each one of them briefly below.

3.5.2. Calculations of the Measured Energy-Efficiency Data with NASEFFICAL

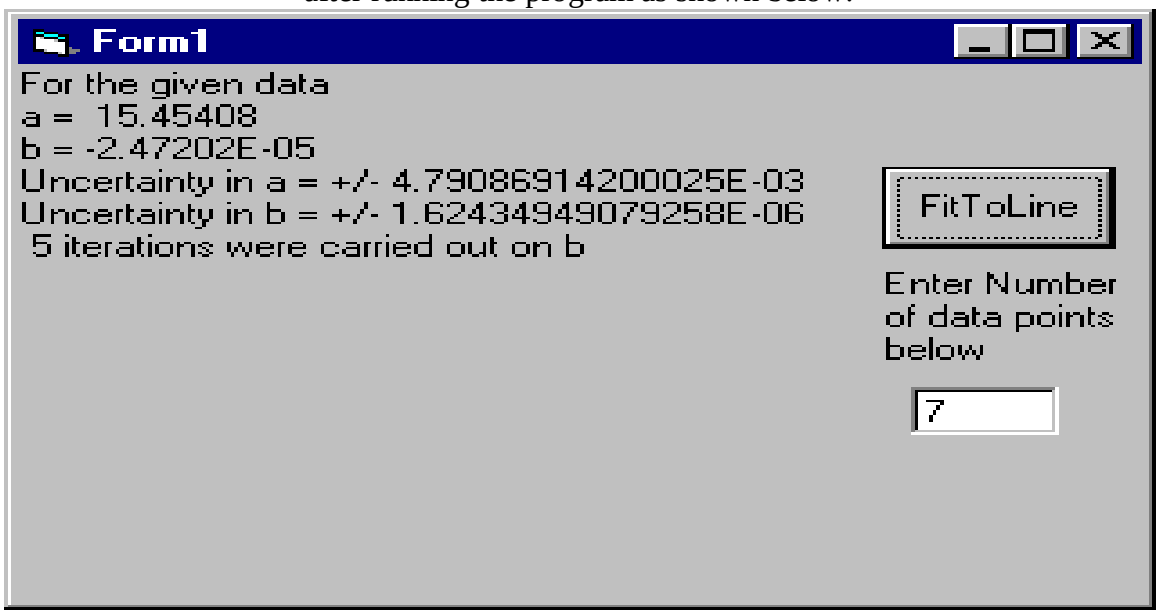
This program simplified the steps involve in Section (3.3.3) of this project. The program stores the efficiency data within a single run, arrange them in order of increasing energy as usually required. It then prints them all into a specified output file. This file can easily serve as input for the fitting program in Section (3.5.4).



3.5.3. Linear Regression With Uncertainty On Both Coordinates (NASLINREG)

Calculations of the propagated uncertainty in τ, requires a program because of the iteration required. For a straight line of the form Y = a + b X the coefficients 'a' and 'b' are the Y-intercept and slope respectively. In the case under consideration, we need to calculate the uncertainties on both axes. Iterations must be carried out on b (York et al 2004) in which case simple regression cannot work (William et al 1992). A typical sequence of operation for obtaining a, b, σ_a and σ_b outlined in the work of York et al is one of the best and most recent ways, though it requires simple regression and correlation coefficient which this work has covered with the aid of the steps given in the book on Mathematical Physics (Gupta, B. D. 1993). The symbol σ_i signifies uncertainty in i.

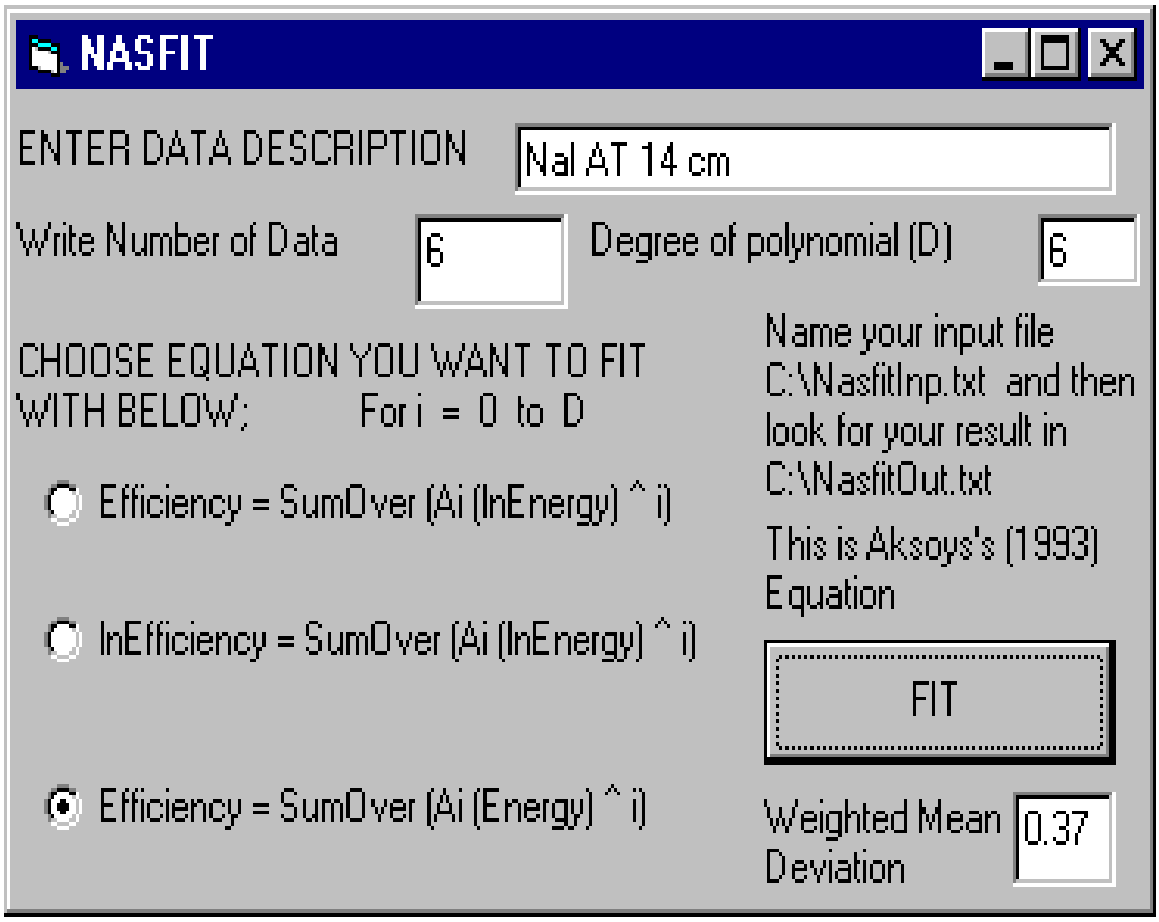
The regression coefficients and their respective uncertainties are displayed on the form after running the program as shown below:



3.5.4. Fitting A Polynomial Function To The Energy-Efficiency Data (NASFIT).

A program named NASFIT was written in Visual Basic Language to fit an arbitrary polynomial to the resulting data from NASEFFICAL, using Gauss Jordan Elimination Method with Maximization Of Pivot, it then returns the fitting coefficients to an output file, as shown in Appendix I.

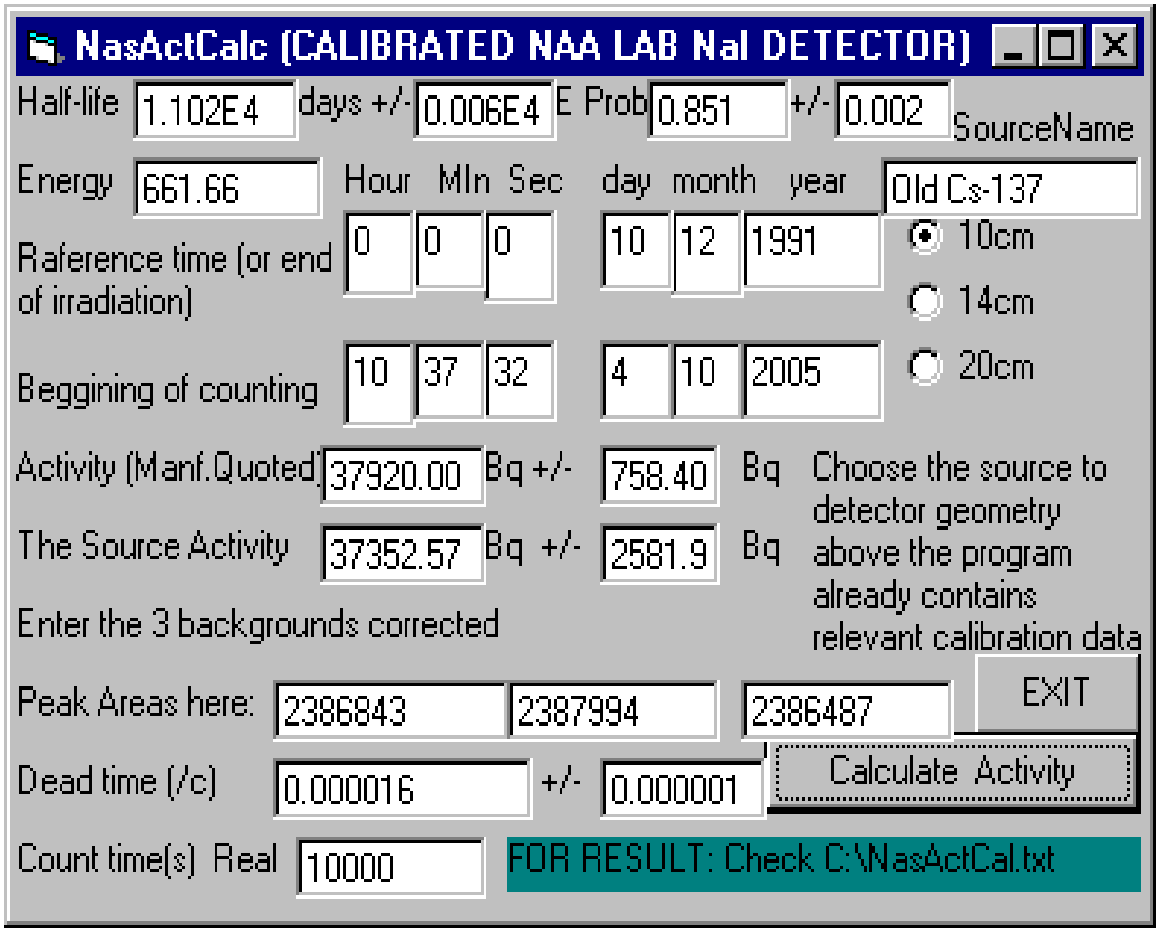
The form layout for this program is shown below:



3.5.5. Activity calculation with (NasActCal)

NASEFFICAL was modified to arrive at a simple calculator for the calibrated geometries of the calibrated spectrometre. All that is need is to fill a simple form with relevant source data and choose the level (counting geometry) used and a click of a button to calculate the activity of the gamma sourcein question. The program prints all the work of a single running in an output file, whose name has been given on the form.

The form is shown below:


NasActCalc (CALIBRATED NAA LAB NaI DETECTOR)
Half-life
1.102E4
days +/-
0.006E4
E Prob
0.851
+/-
0.002
SourceName
Energy
661.66
Hour
Mln
Sec
day
month
year
Old Cs-137
Raference time (or end of irradiation)
0
0
0
10
12
1991
10cm
14cm
20cm
Beggining of counting
10
37
32
4
10
2005
Activity (Manf.Quoted)
37920.00
Bq +/-
758.40
Bq
Choose the source to detector geometry above the program already contains relevant calibration data
The Source Activity
37352.57
Bq +/-
2581.9
Bq
Enter the 3 backgrounds corrected
Peak Areas here:
2386843
2387994
2386487
EXIT
Dead time (/c)
0.000016
+/-
0.000001
Calculate Activity
Count time(s) Real
10000
FOR RESULT: Check C:\NasActCal.txt

CHAPTER FOUR

EXPERIMENTAL SETTINGS AND MEASUREMENT RESULT

4.6 INTRODUCTION

In this chapter, we present the experimental settings used for this work and how they were chosen or arrived at, starting form pole zero adjustment, detector-working voltage, counting geometry and energy calibration. We also briefly describe spectral data acquisition and analysis. The results from the dead time experiment used for the efficiency-energy calibration calculations together with the plot comparing the experimental efficiency points and the analytical functions are well documented. Finally, a table displaying results for two test sources whose gamma ray intensities were determined based on this work's calibration, converted to disintegration rates and compared to the quoted one by their manufacturer.

4.7 THE SPECTROMETRE SET-UP

4.7.1 Initial Adjustments

Pole Zero Cancellation

The pole zero adjustment was carried out on the spectrometre with the aid of an oscilloscope, until a fine Gaussian peak was observed using a ^{137}Cs peak.

Working Voltage Optimization

Varying the voltage and obtaining the count rate in the spectrum optimized the working voltage of the spectrometer. Then the result were plotted and the mid of the plateau for the curve is found to be at 950 Volts as it can be seen in the figure 4.1 below.

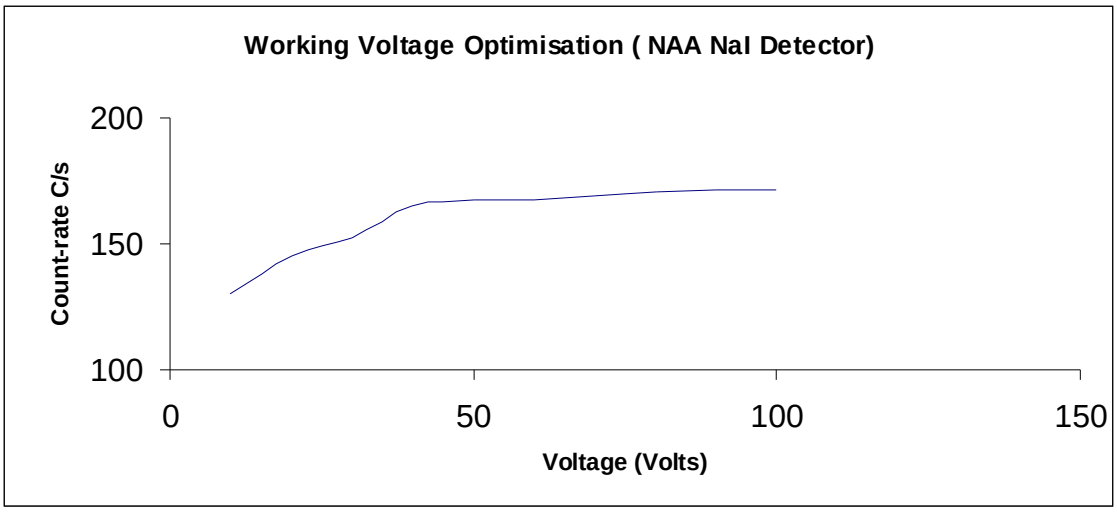


Figure 4.1: A plot of count-rate versus voltage for the detections system

4.7.2 Counting Geometry

A sample holder was designed and constructed to create a reproducible counting geometry, which was used in varying the source-detector distances.

The sample holder was well designed to be portable and durable, as well as having marked positions (source-detector distances). Perspex was chosen as material for the construction, while the sample holder is a bracket type.

The bracket constitutes of rectangular case whose circular base can sit of the cylindrical top of the detector. The side face allows the sample to be slotted, which is to be placed on a provision at the centre of a rectangular plate (sample-slot), which is slotted at various fixed positions in order to vary the source-detector distance. It can fit in to all the available shields around.

The slot-positions were made in such a way that, their separation provides significant intensity change. The variation of intensity of a source with its distance from the detector was investigated, based on the assumption that, the solid angle through which the radiation reaches the detector is proportional to the intensity of the radiation.

The solid angle is related to the distance by equation (3.3.18), whose typical plot is shown in figure 4.2 below:

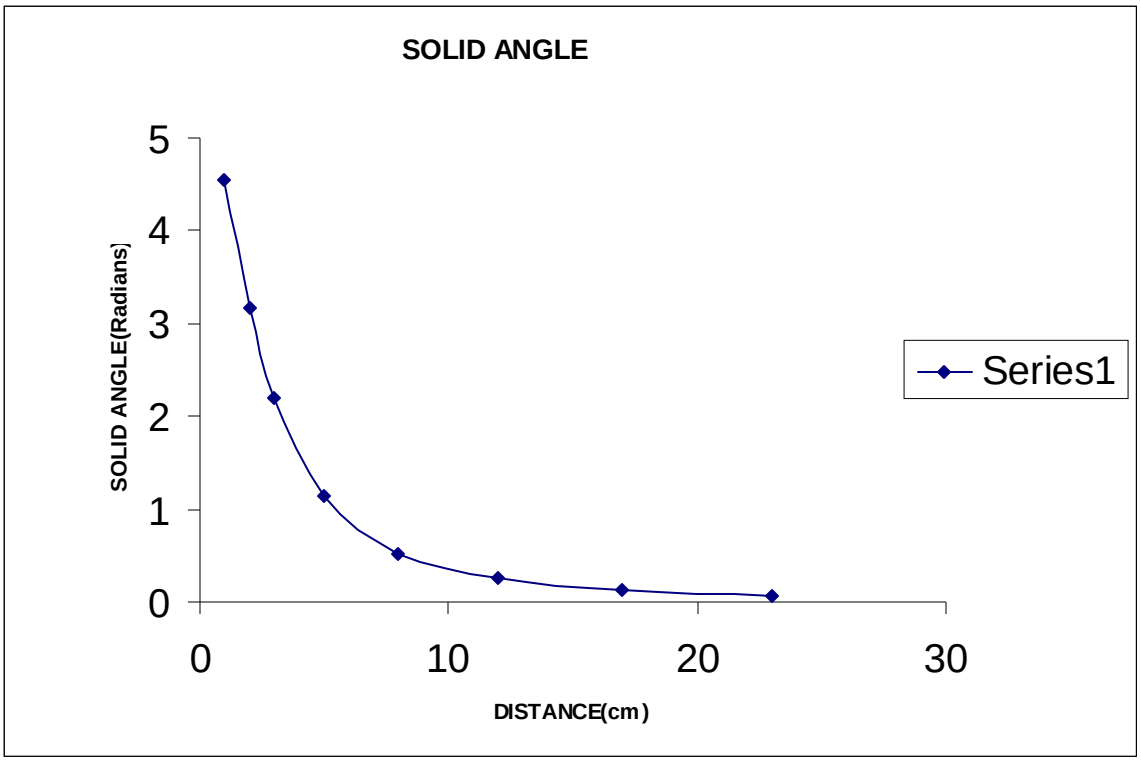


Figure 4.2: Variation of Solid Angle with Source-Detector distances

The above plot shows that, the solid angle Ω varies slightly far away from the detector, hence the intensity. Therefore, the slot positions are close near the detector and more spaced far away.

The whole dimension of the bracket is chosen to allow a reasonable distance to be achieved and also to fit in to the shield. The diagram of the designed sample holder is shown in figure 4.3 below:

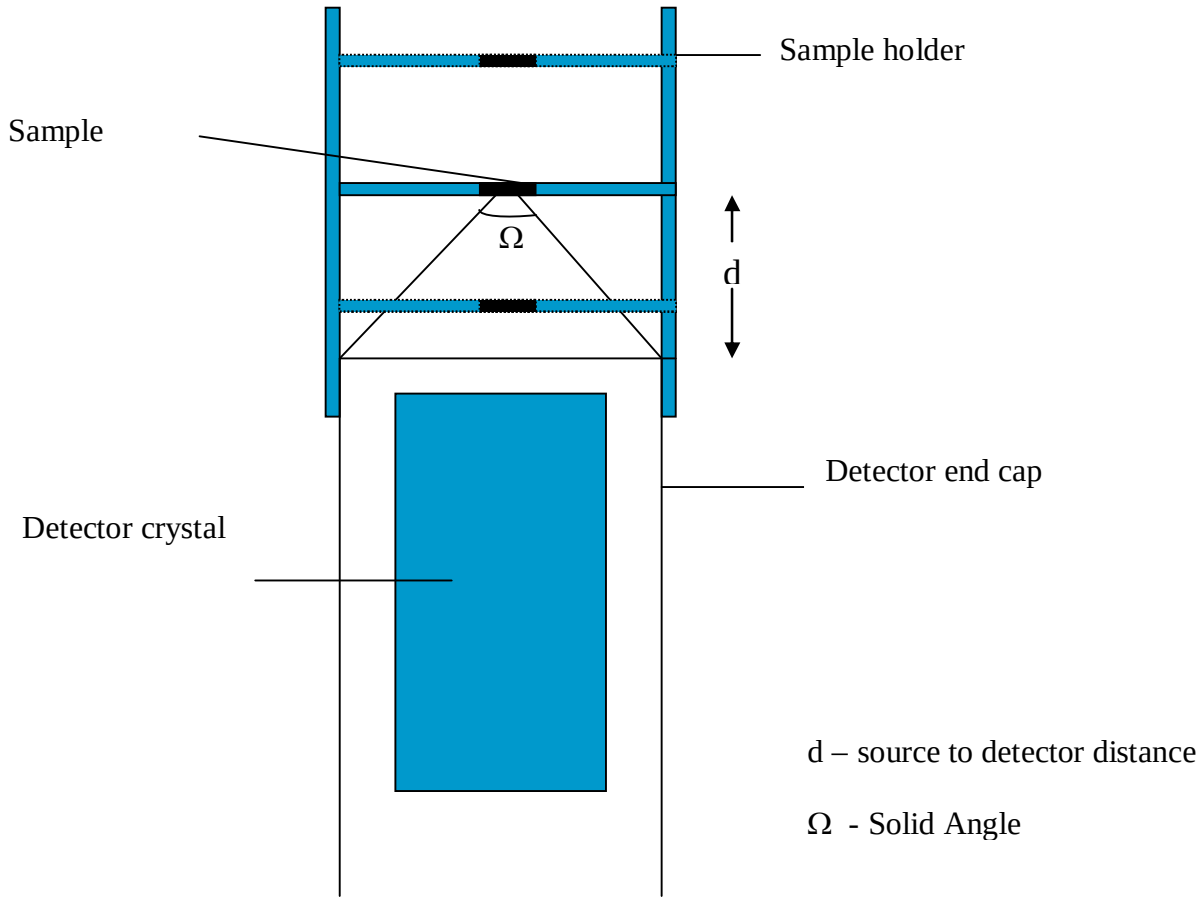


Figure 4.3: The cross section of the Source-Detector geometry established

The counting positions are chosen to be; ten, fourteen and twenty centimeters (10 cm, 14 cm and 20 cm) from the detector surface the positions where true coincidence summation is negligible.

4.7.3 Energy Calibration

The energy-channel calibration was achieved with two sources, Cobalt-60 and Caesium-137 to assist in locating subsequent peaks.

4.8 Spectral Acquisition and Analysis

4.8.1 Introduction

At each of the three chosen geometries, spectra were acquired for the seven standard sources available, the two test sources and three backgrounds (at beginning, half way and end of the experiment). The counting time was chosen long enough to reduce statistical uncertainty. The acquired files were then given coded name for easy identification

4.8.2 Determination of Full Energy Peak Areas using BACKGROUND STRIP METHOD

To analyse the spectrum the following steps were followed:

1. the acquired spectra were recalled from buffer
2. they were then stripped off a background spectrum, using the MAESTRO, by selecting Calculate/Strip and then selecting one of the pre-acquired background spectrum
3. all channels under the desired photo peak were then highlighted (red) as Region of Interest (ROI), using F2, Alt M or ROI/Mark and the right arrow, the selected range noted.
4. simple click on the shaded area with the computer mouse will give the ROI report, which gives Gross and net area under the peak.

5. the gross was recorded since background has been subtracted.
6. Step 2 to 5 were repeated for other two background spectra, acquired at different times, during the work
7. The average of the three results was taken as the background corrected count. This is what a computer program NASEFFICAL use together with some information for further corrections and calculations

4.9 Efficiency Calibration

4.9.1 Dead time per counting event

Results and Discussions

The values of the Natural Logarithms of the Peak Area under the Cs-137 Peak (ln(*A*)) and corresponding Mean Count Rate (*R*) with their respective uncertainties for one of the optimized experiments are shown in the table of values in appendix III.

The values of the coefficients obtained from the program are:

$a = 14.965112 \pm 9.1615 \times 10^{-3}$

$b = -3.227033 \times 10^{-5} \pm 1.9980 \times 10^{-6}$

From the theory;

$\text{Slope} = b = -2\tau$

which implies that

$\tau = (16.135165 \pm 0.99) \times 10^{-6}$

Approximately, $\tau = (16 \pm 1) \times 10^{-6}$ seconds

$\tau = (16 \pm 1)\ \mu s$

The best straight line fitted to the above data and the distribution of the experimental data around it is shown in figure 4.4 below:

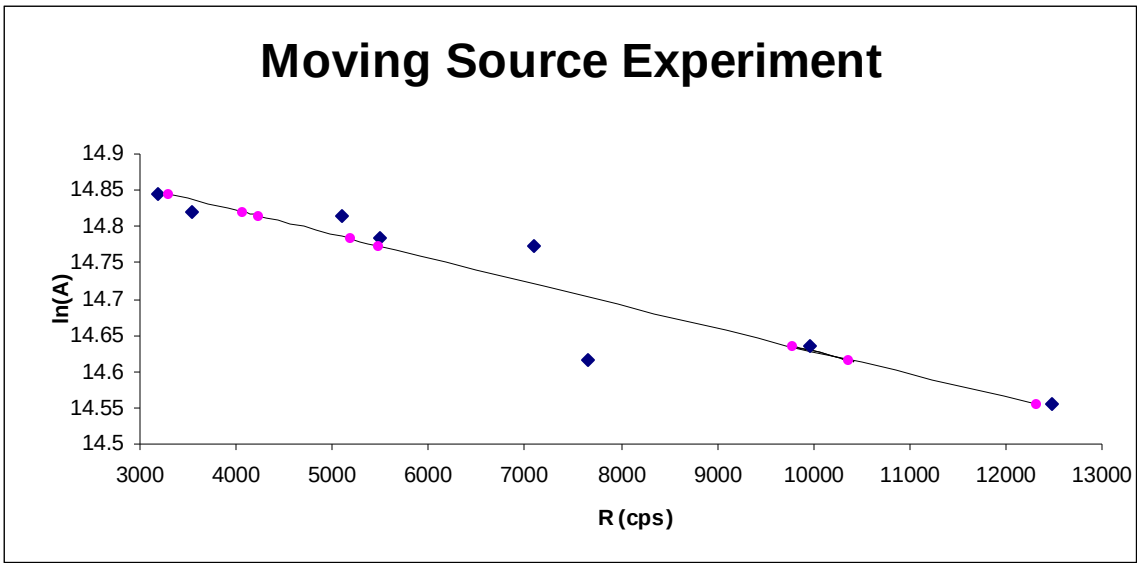


Figure 4.4**:** The plot of natural logarithm of the peak area A with increased total spectral count-rate R as scattered while the smoothed is the fitted equation, whose coefficient where found

4.9.2 Measured Energy-Efficiency Data

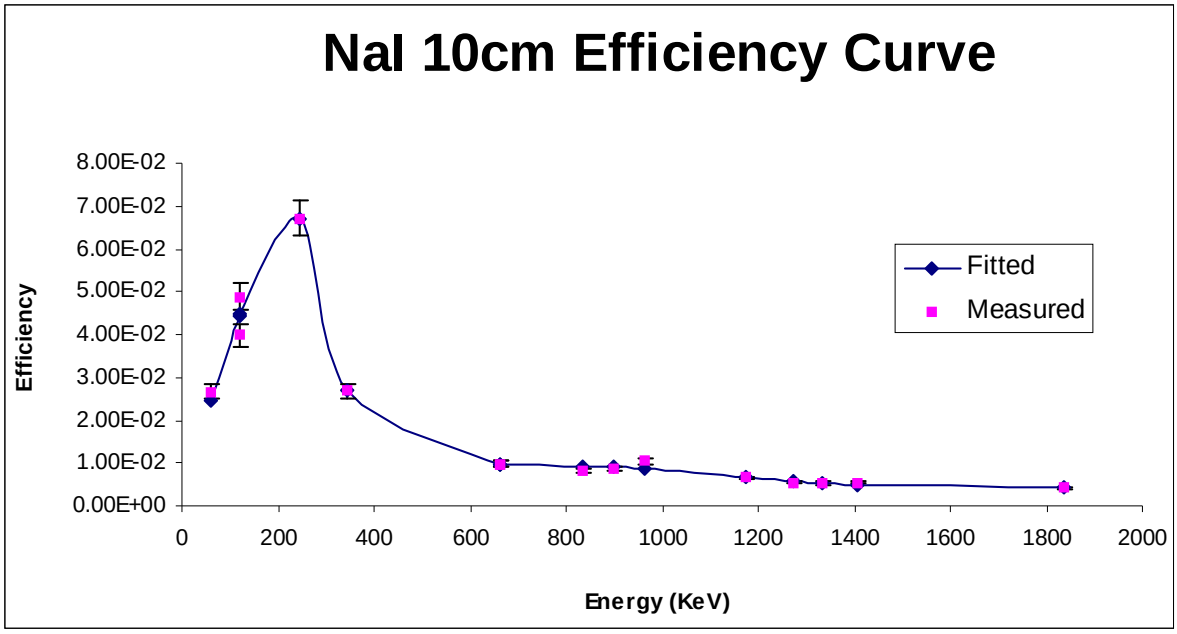
NASEFFICAL is the computer program written, capable of accumulating report on the peak energy, calculated efficiency, propagated uncertainty in calculated efficiency of the entered data at a period, for as many peaks as possible, sort them in the order of ascending peak energies, as well as print them in to a text file. It was used to calculate fourteen efficiency points for the available sources.

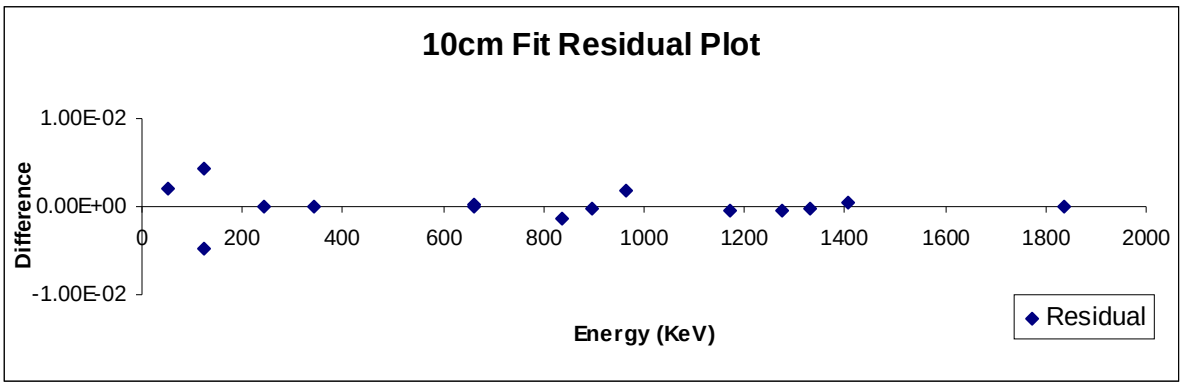
4.9.3 Analytical Function Generation (Theoretical Model)

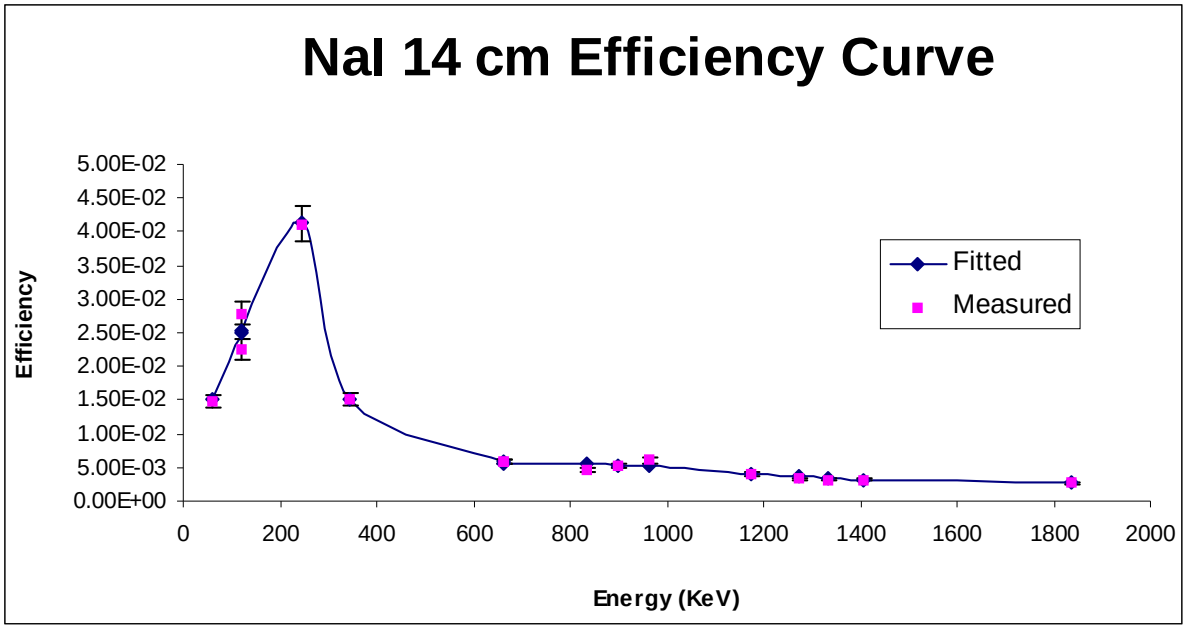
The text files generated by NASEFFICAL were used to prepare input files for NASFIT, the program capable of reading and fitting the data to an equation in the form of arbitrary polynomial. It returns fitting coefficients (for determining the fitted equation), peak energies, in addition to calculated and measured efficiencies together with their weighted mean deviation.

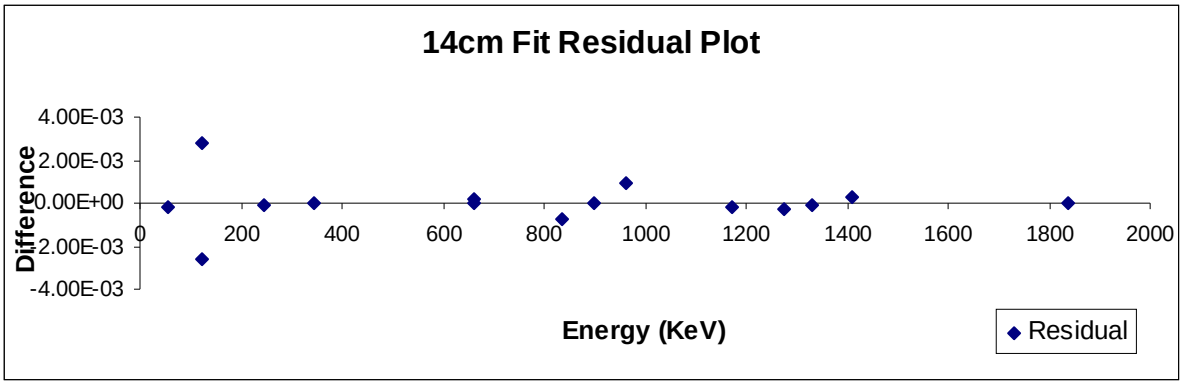
4.9.4 The Calibration Result

The raw result is shown in Appendix I, while below are the plots comparing the energy-efficiency functions and the corresponding measured energy-efficiency data points, for the three source-to-detector geometries considered.






NaI 14 cm Efficiency Curve
Efficiency
5.00E-02
4.50E-02
4.00E-02
3.50E-02
3.00E-02
2.50E-02
2.00E-02
1.50E-02
1.00E-02
5.00E-03
0.00E+00
0
200
400
600
800
1000
1200
1400
1600
1800
2000
Energy (KeV)
Fitted
Measured


14cm Fit Residual Plot
Difference
4.00E-03
2.00E-03
0.00E+00
-2.00E-03
-4.00E-03
0
200
400
600
800
1000
1200
1400
1600
1800
2000
Energy (KeV)
Residual

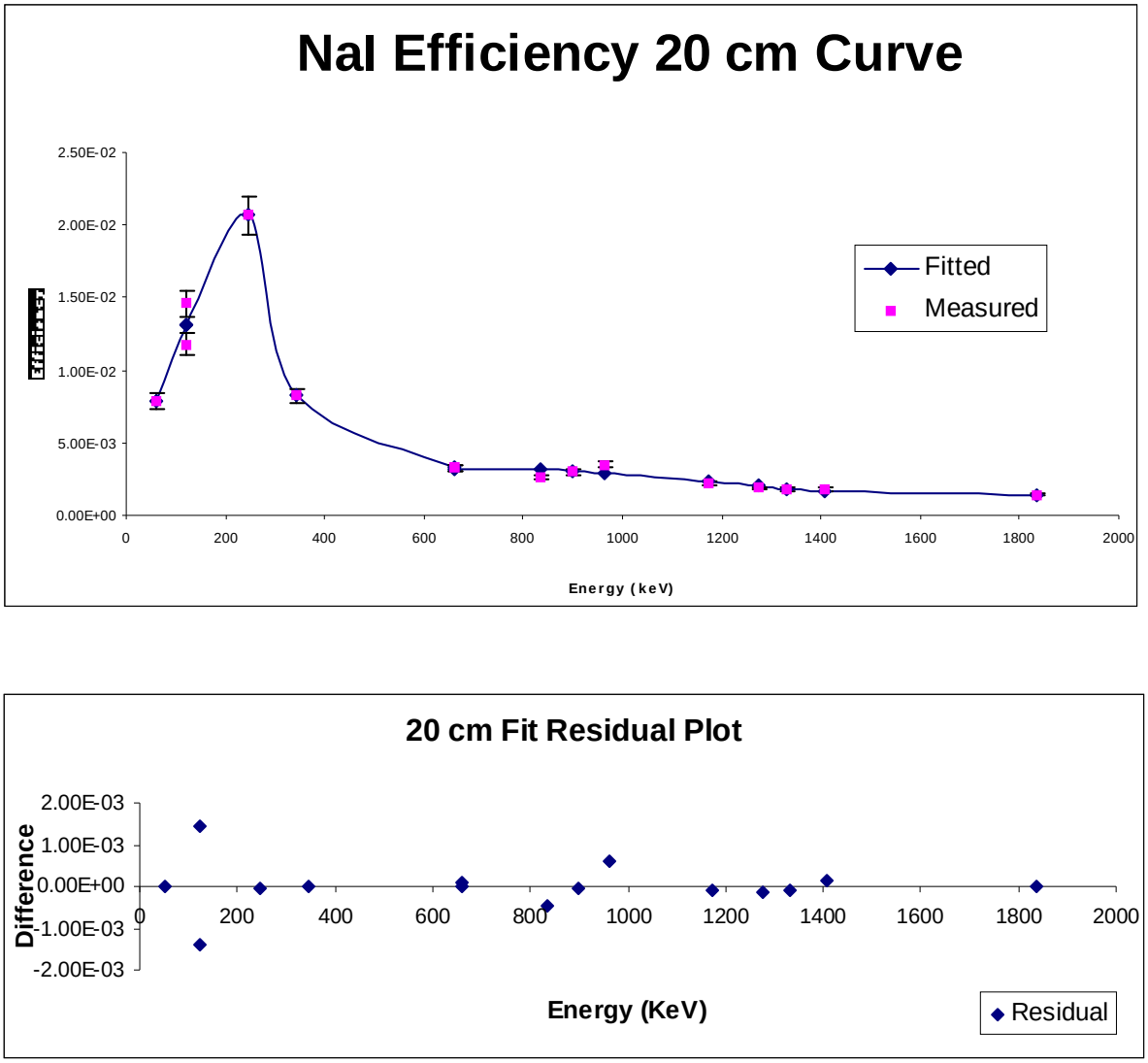


Figure 4.5: The plots of the measured energy-efficiency data in comparison with the energy-efficiency function at various geometry levels

4.10 Determined Disintegration rates of Test Sources

4.10.1 Introduction

The best-generated efficiency function for the three levels calibrated, whose uncertainty was assigned using their weighted mean deviation, are integrated into the intensity

equations (3.3.21) and (3.3.22), to calculate the intensities of gamma energies of two test sources (old standards Sources)

The calculations were done with the computer program, NASACTCAL, described in section 3.5.5 of this report. The peak data were obtained from IAEA –TECDOC-619). For non-standard sources, Atomic Data and Nuclear Data Tables can be used (Reus, 1983).

4.10.2 The Disintegration Rate Determination Result

The accuracy of this work was tested, by using the calibrated system to measure the activity of a known ^{137}Cs source and a ^{60}Co source whose activity was in doubt because it was damaged. The two sources were measured and their activities determined as in the table below.

For comparison, all the activities were determined at the same reference time; the manufacturer's reference time (00:00:00 10/12/1991) was chosen.

SOURCE No 1 (Old ^{137}Cs)		
MANUFACTURER'S QUOTED ACTIVITY (Bq): 37920 ± 758		
ACTIVITY (Bq) DETERMINED USING PEAK ENERGY: 661.66 KeV		
GEOMETRY	ACTIVITY	UNCERTAINTY (±)
Level-3 10cm	38308	2647
Level-2 14cm	36448	2488
Level-1 20cm	37613	2592
AVERAGE	37456	2576

Table 4.1: Table presenting the result of determined activity of an Old ^{137}Cs source

It could be seen from table (4.1) that for ^{137}Cs there is no discrepancy in the result, and the values are consistent.

SOURCE No 2 (Old ^{60}Co)		
MANUFACTURER'S QUOTED ACTIVITY (Bq): 48270 ± 965		
ACTIVITY (Bq) DETERMINED USING PEAK ENERGY: 1173.238 KeV		
GEOMETRY	ACTIVITY	UNCERTAINTY (±)
Level-3 10cm	33081	2285
Level-2 14cm	30960	2113
Level-1 20cm	33152	2284
AVERAGE	32398	2227
ACTIVITY (Bq) DETERMINED USING PEAK ENERGY: 1332.502 KeV		
GEOMETRY	ACTIVITY	UNCERTAINTY (±)
Level-3 10cm	32524	2247
Level-2 14cm	30733	2097
Level-1 20cm	27466	1893
*AVERAGE	30241	2079
**GRAND AVERAGE	31319	2153

Table 4.2: Table presenting the result of determined activity of an Old ^{60}Co source

* AVERAGE - AVERAGE BASED ON GEOMETRY VARIATION
** GRAND AVERAGE – AVERAGE BASED ON GAMMA ENERGIES USED

The activity of the damaged ^{60}Co source was determined to be (31319 ± 2153) Bq, so that it can henceforth be used as a standard gamma ray source.

CHAPTER FIVE

SUMMARY, CONCLUSION AND RECOMMENDATIONS

The NaI(Tl) spectrometer in the NAA laboratory of the Centre for Energy Research and Training (CERT) Ahmadu Bello University, has been setup for accurate determination of sources disintegration rates, as energy-efficiency calibration has been done for measurements at 10 cm, 14cm and 20cm source-detector distances.

In the process a method has been developed for the accurate determination of the dead time using the spectrometer based on the moving source method. A recent method of error propagation by York et al, (2004) was used to assign uncertainty to the dead time, which greatly improved the moving source method.

Relevant calculations have been simplified using computer programs written in Visual Basic 5.0, which are user friendly as they display feedback on the form as well as print results to text files for subsequent utilization. The programs have built-in protections to check common mistakes such as accidental reset, exit or insufficient data supply.

The energy-efficiency has been incorporated in a program NASACTCAL in order to serve as a tool that will ease subsequent utilization of the NaI(Tl) spectrometer, for the accurate determination of source disintegration rates (activities).

All the programs are designed to be flexible so that, they can serve as tools in their respective areas. For instance, NASEFFICAL in efficiency calculations, NASLINREG in all linear regression analysis calculations, NASFIT in fitting equations in the form of arbitrary polynomial to data and lastly NASACTCAL for activity calculations of similarly calibrated spectrometers.

The work has accurately determined the new absolute activity of a damaged Cobalt (^{60}Co) standard source using the NaI(Tl) spectrometer. This source can still be used as a standard source when required.

Recommendations

1. The project recommends a similar work be carried out on all the spectrometers in CERT, so that users need not to worry about the energy-efficiency calibration, and the process should be repeated periodically (say biannually). Since the active volume of the detectors may change with time.
2. In future, further comparison should be undertaken between this method and the commonly used relative method, so as to reduce the fear of exhausting the limited standards at hand.

3. The fact that the project considered time in seconds, and took good care of the time in the computer used, synchronization of clocks relative to GMT should be a routine in all counting stations in CERT. This assisted in converting the reference time of the standard sources used from PST to GMT and then to local time.

REFERENCES

Aksoy, A.; (1993): Efficiency Calibration of the HPGe Detector in Far and Close Geometries; Journal of Radioanalytical and Nuclear Chemistry, Volume 109 No 2; Elsevier Sequoia S. A., Lausanne Akademai Kiado, Budapest. PP (463 – 469)

Bevington Philip R. and D. Keith Robinson; **(**Second Edition, 1992): Data Reduction And Error Analysis For The Physical Sciences; WCB/McGraw-Hill. PP (38 – 48)

Debertin, K. and Helmer, R.G.; (1988): Gamma- and X –ray Spectrometry with semiconductor detectors; Elsevier Science Publishers B.V., The Netherlands. PP (29 – 287)

Debertin, K., Schotzig U., Walz K. F., and Weiβ, H.; (1976): Efficiency Calibration of semiconductor spectrometers Techniques and Accuracies; Prooceedings, ERDA X-ray and Gamma-Ray Symp. Ann Arbor,MI, May 19 – 21, (Conf 760539). PP (59–62)

EG&G ORTEC; (1995): Modular Pulse –Processing Electronics and Semiconductor Radiation Detectors; EG&G ORTEC, U.S.A. PP (36 – 293)

Ewa I. O. B., Bodizs D., Czifrus Sz. and Molnar Zs.;(2001): Monte Carlo determination of full energy peak efficiency for a HPGe detector; Applied Radiation and Isotopes (Journal); Elsevier Science Ltd. PP (103 – 108)

Frank, H and Althoen S.C.; (Low priced Edition (1995) Reprint (2002)): Statistics Concepts and Application; Press Syndicate of the Cambridge University Press, United Kingdom. PP (98 – 147, 570 – 609)

Gupta B. D.;(Second Revised Edition (2002)): Mathematical Physics; Vikas Publishing House PVT LTD, New Delhi. PP (15.128 – 15.149)

Gilmore Gordon and John Hemingway; **(**1995): Practical Gamma-ray Spectrometry; John Wiley & Sons, England. PP (22 – 27, 128 – 159, 183 – 224))

Gunnink R.and Prindle A.L. (1991): Non-conventional Methods for accurately calibrating Germanium Detectors; Lawrence Livermore National Laboratory. PP (1 – 12)

Gunnink R.; (1990): New Method For Calibrating a Ge Detector Using Only Zero to Four Efficiency Points; Elsevier Science Publishers B.V.. North-Holland.

IAEA (1991): X-ray and gamma-ray standards for detector calibration; IAEA-TECHDOC-619; IAEA Vienna Austria. PP (149 – 156)

IAEA (2001): Quality aspects of research reactor operations for instrumental neutron activation analysis (Report of an advisory group meeting held in Accra, Ghana 18th to 22nd October 1999; IAEA-TECDOC-1218; IAEA Vienna Austria. PP (14 – 20)

Jenkins Ron, Gould R. W. and Dale Gedcke; (1981): Quantitative X-Ray Spectrometry; Marcel Dekker Inc. New York, U.S.A. PP (229 – 275)

Jonah S. A. and Zakari I. Y.; (2000): Variation of Efficiency Curve of a NaI(Tl) Detector with Source Detector Distance; Conference Proceedings of the 23rd Annual Conference of the Nigerian Institute of Physics " The Millenium Conference". PP (83 – 84)

Knoll Glenn F; (Second Edition, 1979): Radiation Detection And Measurement John Wiley and Sons. PP (39 – 349)

Kreyszig Erwin; (Seventh Edition (1993)): Advanced Engineering Mathematics; John Wiley & Sons, Inc. Singapore. PP (365 – 367)

Osae E. K.; Nyarko B. J. B.; Serfo-Amara Y.; Darko E. O.;(1999); An empirical expression for the full peak efficiency of an N-type high purity germanium detector; Journal of

Radioanalytical and Nuclear Chemistry, Vol.242 No. 3; Elsevier Science B.V. Amsterdam, Akademai Kiado, Budapest. PP (617 – 622)

Reus U. and Westmeiser W.; (1983): Catalog of gamma rays from radioactive decay part II; Academic Press Inc. U.S.A.

Taylor John R.; **(**Second Edition 1997): An Introduction To Error Analysis (The study of uncertainties in measurements); University Science Books, California. PP (389 – 394)

Usman K.;(2000): Precise measurement of the half lives and emission probabilities of ^{233}Th and ^{233}Pa; PhD thesis, Imperial College, London. PP (40 – 61)

William H. P., Saul A.T., William T.V. and Brian P.F.; (Second Edition (1992)): Numerical Recipes in C; Cambridge University Press. PP (36 – 41)

York Derek, Evensen N.M., Martinez M. L. and Delgado J.; (2004): Unified Equations For The Slope And Intercept And Standard Error Of The Best Straight Line; American Association Of Physics, American Journal Of Physics 72 (3) March 2004. PP (367 – 375)

APPENDICES:

APPENDIX I: FITTING NaI EFFICIENCY CALIBRATION DATA WITH AKSOY'S (1993) EQUATION

****
********** **FIRST REGION (59.537 TO 661.660) KeV**********
****

THE FIT RESULT OF NaI AT 10 cm

THE COEFICIENTS OF THE FITTED EQUATION
A 0 = 2.021398E-02
A 1 = -1.179245E-04
A 2 = 3.592632E-06
A 3 = -4.204719E-09
A 4 = -4.434535E-11
A 5 = 1.090815E-13
A 6 = -6.699031E-17

Equation Used: Aksoy's (1993) Equation

The Fitted equation is shown below:
Eff = 0.0202 - 0.000118 (Eg) + 3.59E-06(Eg)^ 2 - 4.20E-09(Eg)^ 3 - 4.43E-11(Eg)^ 4 + 1.09E-13(Eg)^ 5 - 6.70E-17(Eg)^ 6
Where: Eff - is the Efficiency and Eg - is the Gamma Energy

The Weighted Mean Deviation is 0.42%

Energy	Calculated	Measured	Uncertainty
59.537	2.456182E-02	0.0265782	1.687841E-03
121.7824	4.448999E-02	4.884367E-02	3.061279E-03
122.0614	0.0445901	3.977422E-02	2.487457E-03
244.6989	6.719457E-02	6.713396E-02	4.211673E-03
344.2811	2.690471E-02	2.694015E-02	1.687685E-03
61.66	9.841447E-03	9.839674E-03	6.155033E-04

****

THE FIT RESULT OF NaI AT 14 cm

THE COEFICIENTS OF THE FITTED EQUATION
A 0 = 1.249958E-02
A 1 = 7.887454E-06
A 2 = 5.427088E-07
A 3 = 5.393207E-09
A 4 = -3.195391E-11
A 5 = 3.400733E-14

Equation Used: Aksoy's (1993) Equation

The Fitted equation is shown below:
Eff = 0.0125 + 7.89E-06 (Eg) + 5.43E-07(Eg)^ 2 + 5.39E-09(Eg)^ 3 - 3.20E-11(Eg)^ 4 + 3.40E-14(Eg)^ 5
Where: Eff - is the Efficiency and Eg - is the Gamma Energy

The Weighted Mean Deviation is 0.37%

Energy	Calculated	Measured	Uncertainty
53.537	1.505739E-02	0.0148713	9.444236E-04
121.7824	2.513241E-02	2.792153E-02	1.750016E-03
122.0614	2.518449E-02	2.256596E-02	1.480053E-03
244.6989	4.121723E-02	4.110891E-02	2.579095E-03
344.2811	1.518669E-02	1.522873E-02	9.540506E-04
661.66	5.844293E-03	5.843511E-03	3.65541E-04

****

THE FIT RESULT OF NaI AT 20 cm

THE COEFICIENTS OF THE FITTED EQUATION
A 0 = 1.110608E-02
A 1 = -1.723459E-04
A 2 = 2.459922E-06
A 3 = -8.376722E-09
A 4 = 7.595257E-12

Equation Used: Aksoy's (1993) Equation

The Fitted equation is shown below:
Eff = 0.0111 - 0.000172 (Eg) + 2.46E-06(Eg)^ 2 - 8.38E-09(Eg)^ 3 + 7.60E-12(Eg)^ 4
Where: Eff - is the Efficiency and Eg - is the Gamma Energy

The Weighted Mean Deviation is 0.38%

Energy	Calculated	Measured	Uncertainty
59.537	7.892324E-03	7.872867E-03	5.000064E-04
121.7824	0.0131414	1.458029E-02	9.138742E-04
122.0614	1.317181E-02	1.176594E-02	7.35873E-04
244.6989	2.072329E-02	0.0207	1.298824E-03
344.2811	8.218749E-03	8.228894E-03	5.155625E-04
661.66	3.253159E-03	3.252866E-03	2.034946E-04

****

* **SECOND REGION (661.660 to 1836.063) KeV** **********
****

THE FIT RESULT OF NaI AT 10 cm

THE COEFICIENTS OF THE FITTED EQUATION
A 0 = -4.35765E-03
A 1 = 4.556411E-05
A 2 = -4.550057E-08
A 3 = 1.264029E-11

Equation Used: Aksoy's (1993) Equation

The Fitted equation is shown below:
Eff = -0.00436 + 0.0000456 (Eg) - 4.55E-08(Eg)^ 2 + 1.26E-11(Eg)^ 3
Where: Eff - is the Efficiency and Eg - is the Gamma Energy

The Weighted Mean Deviation is 0.90%

Energy	Calculated	Measured	Uncertainty
661.66	9.531947E-03	9.839674E-03	6.155033E-04
834.843	9.323832E-03	7.968544E-03	4.981678E-04
898.042	9.02032E-03	8.756502E-03	5.482535E-04
964.055	8.605967E-03	1.051742E-02	6.589625E-04
1173.238	6.882335E-03	6.514164E-03	4.071964E-04
1274.542	5.972937E-03	5.453628E-03	3.409166E-04
1332.502	5.473712E-03	5.227807E-03	3.267897E-04
1408.022	4.876169E-03	5.426939E-03	3.401278E-04
1836.063	4.151069E-03	4.133637E-03	2.585633E-04

THE FIT RESULT OF NaI AT 14 cm

THE COEFICIENTS OF THE FITTED EQUATION
A 0 = -2.314919E-03
A 1 = 2.63711E-05
A 2 = -2.652243E-08
A 3 = 7.423694E-12

Equation Used: Aksoy's (1993) Equation

The Fitted equation is shown below:
Eff = -0.00231 + 0.0000264 (Eg) - 2.65E-08(Eg)^ 2 + 7.42E-12(Eg)^ 3
Where: Eff - is the Efficiency and Eg - is the Gamma Energy

The Weighted Mean Deviation is 0.78%

Energy	Calculated	Measured	Uncertainty
661.66	5.672853E-03	5.843511E-03	3.65541E-04
834.843	5.535174E-03	4.749013E-03	2.969087E-04
898.042	5.354273E-03	5.355309E-03	3.353666E-04
964.055	5.109864E-03	6.019916E-03	3.772381E-04
1173.238	4.105744E-03	3.929997E-03	2.456709E-04
1274.542	3.581909E-03	3.326865E-03	2.079791E-04
1332.502	3.29643E-03	3.17755E-03	1.986374E-04
1408.022	2.957565E-03	3.218875E-03	2.017824E-04
1836.069	2.643333E-03	2.636176E-03	1.65175E-04

THE FIT RESULT OF NaI AT 20 cm

THE COEFICIENTS OF THE FITTED EQUATION
A 0 = -1.95045E-03
A 1 = 1.63576E-05
A 2 = -1.599157E-08
A 3 = 4.399522E-12

Equation Used: Aksoy's (1993) Equation

The Fitted equation is shown below:
Eff = -0.00195 + 0.0000164 (Eg) - 1.60E-08(Eg)^ 2 + 4.40E-12(Eg)^ 3
Where: Eff - is the Efficiency and Eg - is the Gamma Energy

The Weighted Mean Deviation is 0.86%

Energy	Calculated	Measured	Uncertainty
661.66	3.146123E-03	3.252866E-03	2.034946E-04
834.843	3.119934E-03	2.642497E-03	1.652281E-04
898.042	3.028858E-03	2.992168E-03	1.874641E-04
964.055	2.898532E-03	3.492584E-03	2.189259E-04
1173.238	2.333715E-03	2.223772E-03	1.39022E-04
1274.542	2.029324E-03	1.867007E-03	1.16728E-04
1332.502	1.861076E-03	1.790847E-03	1.11961E-04
1408.022	1.658718E-03	1.81866E-03	1.140526E-04
1836.063	1.404815E-03	1.400699E-03	8.77306E-05

****
****END OF FITTTING RESULT WITH AKSOY'S EQUATION****
****

APPENDIX II: DETAILS OF SPECTROMETRE COMPONENTS SPECIFICATIONS

The Sodium Iodide NaI (Tl) Detector

Description;

Model Number: Model 802-4
Serial Number: 8904425
Crystal Assembly: Monoline
Photomultiplier: Model 2007 or 2007P
Crystal Size: 3 in. x 3 in.
RESOLUTION: 7.5%
RESOLUTION: Specified at 662 eV of Cs-137
TUBE SIZE: 3 in.

WINDOW: 0.02 in. aluminum, density 147.9 mg/cm^2
REFLECTOR: Oxide1/16 in. thick, density 88mg/cm^2
MAGNETIC / LIGHT SHIELD: Conetic Lined Steel
TYPICAL OPERATING VOLTAGES:
Cathode to Anode +1100VDC
Dynode to Dynode +80VDC
Cathode to Dynode +150VDC

The Photo Multiplier Tube And Preamplifier

Description:

Model Number: Model 2007P
Serial Number: 12903791

INPUTS

DETECTOR SIGNAL: Preamp input is AC to anode via pin 11
HIGH VOLTAGE: 2kVDC Maximum
TEST: +ve or –ve at 30 picocoulombs/ V, input impedance 93Ω
PREAMP POWER: ±12V DC (amplifier powered)

OUTPUTS

PREAMP SIGNAL: Inverted tail pulse; rise time, < 20ns; fall time, 50μs nominal; up to +10V through series connected 93Ω resistor; direct coupled

CONTROLS

FOCUS: Single turn screwdriver adjustment for optimization of resolution.
GAIN: Single turn screwdriver adjustment for trimming HV

PERFORMANCE

INTEGRAL NON-LINEARITY - <±0.04% for up to +10V
GAIN DRIFT - <±0.01% per ^{o}C (±100ppm / ^{o}C)
PM TUBE BIAS ISOLATION - +2000VDC maximum
NOISE - <0.1femtocoulomb (10^{-6} coulomb)
CHARGE SENSITIVITY - 4.5 mV / picocoulomb, nominal

Divider bias- total resistance 7 ohm., nominal; 10 dynodes @ 72V per k VDC of detector bias; anode limiting resistor 560k ohm.
FOCUS CONTROL RANGE - +72V to +145V per kVDC of detector bias
GAIN CONTROL RANGE - varies total PMT bias from between 92% and100% of the applied voltage.

CONNECTORS

POWER - Amphenol 17 series
TEST – BNC
OUTPUT – BNC
H.V. – SHV
PM TUBE SOCKET – Cinch-Jones 3M-14

POWER REQUIREMENTS

PREAMP - ±12VDC @ 15mA
HV – 0-2k VDC @ 0-300μADC

PHYSICAL

DIAMETRE – 2.3 in. (5.8 cm)
LENGTH – 3 in. (7.6 cm)
NET WEIGHT – 0.5lb (0.2 Kg)
SHIPPING WEIGHT – 2.5lb (1.1 Kg)

The Minibin And Power Supply

The minibin on which sits the modules, contains and ORTEC 402A power supply, having Serial Number: 13279
On a label attached the following are found:

INPUT:	103.129 vac	50 – 65 Hz
	206.259 vac	50 – 65 Hz
OUTPUT:	+12V 2A	-12V 2A
	+24V 1A	-24V 1A
	Max 72 W dc @ 50 ^{o}C	
	115 Vac limited by fuse at 115 Vac	
	Input 50 VA @ 230 Vac Input	

FUSE: 3A @ 115 Vac 1.5A @ 230 Vac

The Detector Bias Supply

It is an EG &G ORTEC Model 428
Specifications:

PERFORMANCE

NOISE AND RIPPLE: <0.0002%.
TEMPERATURE INSTABILITY: <±0.02%/^{o}C, 0 to 50 ^{o}C.
LINE INSTABILITY: Directly proportional to dc power supply instability (<±0.02% for 105 to 125 V ac when using one of the EG &G ORTEC
Model 4002 series power series).

CONTROLS AND INDICATORS

A/B (0 – 1000 V): Front panel 10-turn direct readout potentiometers for bias control.
POS/OFF/NEG: Front-panel switch selects positive and negative output for both detectors.
CURRENT MONITOR Front-panel jacks for accommodating external meter in each output circuit.

OUTPU1TS

A/D SHV connectors on front panel provide short circuit proof outputs for each detector; range 0 – 1000; positive or negative polarity for both detectors impedance ~1.3MΩ.

ELECTRICAL AND MECHANICAL

POWER REQUIRED: +24 v, 165 mA; -24 V, 165 mA.
WEIGHT:
Net 1.82 kg (4.0 lb)
Shipping 3.3 kg (7.25 lb).
DIMENSION: NIM-standard double width module 6.90 x 22.13 cm (2.70 x 8.714 in.) Per DOE/ER-0457T

The Linear Amplifier

EG&G ORTEC model 485 spectroscopy amplifier
Specifications:

PERFORMANCE

SHAPING: Active network filter resulting in approximately Gaussian shape, peak amplitude at 1.5μsec for unipolar and 1.1μsec for double clip; crossover at 2.5μsec for bipolar
MAXIMUM GAIN 640
LINEARITY ±0.15% over specified linear range
NOISE: 10 μV at maximum gain and single clip, 12 μV at maximum gain and double clip, both referred to input.
SHORT-CIRCUIT LIMITS Amplifier will sustain a direct short on the output for an indefinite period for counting rates up to 10^4 Hz
COUNTING RATE: <0.5% gain shift and 0.25% resolution spread FWHM for a pulser peak above a 50,000-count/sec ^{137}Cs background
OVERLOAD: Recovery within 2% of rated output from 600 times overload in 2.5 nonoverloaded pulse widths (25μsec) at maximum gain and specified input
CROSSOVER WALK: ±3 nsec for 10:1 dynamic range with 1 –μsec bipolar shaping (including Amplifier and ORTEC 420 Timing Single Channel Analyzer).
TEMPERATURE STABILITY: 0.02%/^{o}C, 0 to 50 ^{o}C.

CONTROLS

FINE GAIN: Provides a dynamic range of 3:1; selectable from X3 through X10, continuously variable.
COARSE GAIN: A rotary with binary selection covers range of X2 to X64 in 6 steps.
UNIPOLAR-BIPOLAR: Either unipolar or bipolar output pulses are switch selectable. The gains are matched in both modes to ~±2.5%.
PZ-TRIM: A trim potentiometer permits pole zero cancellation network to be adjusted for varying preamplifier decay times.
POS-NEG: A switch to accommodate either positive or negative input signal from a preamplifier.

INPUT

Front panel type BNC connector to preamplifier pulses having either polarity. Input pulses should not have < 0.25μsec rise time for the best filter action**,** 40 μsec minimum decay time for pole-zero cancellation, 12 V maximum, 6 V maximum to prevent saturation before differentiation, 1000Ω impedance, dc-coupled.

OUTPUT

Front panel type BNC connector provides low impedance shaped output, with a test probe adjacent for oscilloscope monitoring. Unipolar or bipolar, 0 to 10 V linear with

11.5 V saturation in to 1000Ω; 0 to 9 V linear with 10 V saturation in to 100Ω;0.50Ω output impedance.

ELECTRICAL AND MECHANICAL

POWER REQUIRED: +24 v, 35 mA; +12 V, 50 mA.
-24 v, 35 mA; -12 V, 70 mA.

WEIGHT:
Net 0.91 kg (2.0 lb)
Shipping 2.27 kg (5.0 lb).

DIMENSIONS: NIM-standard single-width module (1.35 by 8. 174 in.) Per TID-20893 (Rev.).

THE SHIELD

MATERIAL	THICKNESS (cm)
Tin	0.10
Inner Stainless steel	0.50
Copper	0. 05
Annular Lead	4.50
Outer Stainless steel	0.50

APPENDIX III: Table for the Moving Source Experimental Result

S/no	ln(A)	$\sigma_{(\ln(A))}$	(R)	$\sigma_{(R)}$
1	14.84462	0.0005980	3193.698	0.515889
2	14.82026	0.0006050	3537.042	0.542912
3	14.81482	0.0006070	5103.501	0.652144
4	14.78368	0.0006160	5485.851	0.676132
5	14.77426	0.0006190	7104.406	0.769437
6	14.61671	0.0006700	7647.068	0.798283
7	14.63591	0.0006640	9960.026	0.911045
8	14.55381	0.0006910	12479.39	1.019779

Table III Table of values showing the variation of the natural logarithm of the peak area A with increased total spectral count-rate R